2007

Improved corrosion resistant steel for highway bridge construction

Kate Anrico
Lehigh University

Arico, Kate E.

Improved Corrosion Resistant Steel for Highway Bridge Construction

January 2008

Improved Corrosion Resistant Steel for Highway Bridge Construction

by

Kate E. Arico

A Thesis
Presented to the Graduate and Research Committee
of Lehigh University
in Candidacy for the Degree of
Master of Science

in
Industrial Engineering

Lehigh University

January 2008

This thesis is accepted and approved in partial fulfillment of the requirements for the Master of Science.

December 4, 2007
Date

Dr. John H. Gross
Thesis Advisor

Dr. Robert Stout
Thesis Advisor

Dr. Mikell Groover
Faculty Advisor

Chairperson of the Industrial
Engineering Department

ACKNOWLEDGEMENTS

I would like to thank Dr. John Gross and Dr. Robert Stout for their insight, knowledge, and guidance during the course of my research. Dr. Gross, I appreciate everything you have done for me. Thanks is not enough. I would also like to thank Dr. Mikell Groover for his knowledge and assistance throughout my college experience. Additionally, I would like to thank the Federal Highway Administration and ATLSS for the funding required to perform this study at Lehigh University. I would also like to thank my family, Mom, Dad, Tommy, and Kevin, for all their on-going support and love.

Table of Contents

List of Tables

List of Figures

List of Illustrations

Abstract

Highway bridges are predominantly constructed from steel in accordance with the composition and properties adopted by the American Society for Testing and Materials (ASTM) in Specification A709. The A709 steels are used extensively and successfully, but the higher strength steels with yield strengths of 70-100 ksi have undesirably low fracture toughness and commonly require preheat to avoid heat-affected-zone (HAZ) hydrogen-assisted cracking (HAC) during welding. The Lehigh University Center for Advanced Technology for Large Structural Systems (ATLSS) developed a copper-nickel (Cu-Ni) steel with a minimum yield strength of 100 ksi that does not require preheat and possesses excellent toughness. However, all steels are susceptible to atmospheric corrosion, which greatly reduces the life-cycle of these bridges.

To address this problem, the Federal Highway Administration (FHWA) contracted with ATLSS to develop an "Improved Corrosion Resistant Steel" for Highway Bridge construction" that (1) is capable of production on existing American facilities, (2) has the same general performance characteristics as the current A709 steels, (3) is readily weldable using standard welding processes, (4) has enhanced corrosion resistance compared with standard A709 weathering-grade steels, and (5) can be generally competitive in cost with A709 steels. The ATLSS program has adopted a Cu-Ni steel for the base composition and has investigated four chemical composition iterations of the base composition. Within the broad program the subject thesis was assigned the following objectives: (1) develop a regression

analysis relating chemical composition to required mechanical properties, (2) develop a regression analysis relating chemical composition to corrosion performance, and (3) develop an equation for calculating the cost of commercial production of experimental steels based on the cost of alloy additions to the base steel.

The conclusions from the experimental evaluation of the effect of chemical composition resulted in (1) equations for mechanical properties involving the prediction of yield strength, tensile strength, and energy absorption at -40F (-40°C), and (2) a composite equation for predicting corrosion performance based on thickness-loss of the test coupons. These conclusions constitute a methodology for continuing the development of an improved corrosion resistant steel for highway bridge construction and recommend continued experimental approaches.

1. INTRODUCTION

In the United States, interstate and major state highways are crossed by several thousands of bridges. These bridges are constructed from steel or reinforced concrete. Steel is chosen more often than concrete due to its attractive design capability and fabrication flexibility.

1.1 Selection of Existing Steels for Bridges

Highway bridges currently utilize two types of steel—carbon based grades and weathering steel grades. Carbon based steels are prone to rapid rates of corrosion and consequently, they need supplementary protection known as protective coating systems. Weathering steels produce their own protection by forming a rust patina, or film. The formation of this rust layer depends on the environment in which the weathering steel is exposed. An ideal environment is one with "repeated wet-dry cycles and low levels of chloride[1*]." The scope of this project was to find a new steel grade that does not require the use of a protective coating system; therefore, weathering steel grades were considered rather than carbon based steels.

The use of a protective coating system is not a good option because the new steel would increase the cost of the bridge maintenance by labor and material expenses due to periodic recoating. Another reason protective coating systems were avoided was because studies have shown once the coating is damaged (producing "holidays"), the rate of corrosion increases because corrosion is concentrated in a small area[2].

---

* See References

Steels for constructing bridges including highway bridges, are designated by the American Society for Testing and Materials (ASTM) in ASTM Specification A709. This specification covers steels at minimum yield strengths of 36 ksi (A36), 50 ksi (A588), 70 ksi (A852) and 100 ksi (A514). These steels have also been specified for bridges by the American Association of State Highway Officials (AASHO) who have adopted A709 for bridge construction. Although these steels have been used extensively and successfully for highway bridges, the weldability and fracture toughness of many of these steels, particularly those at 80 and 100 ksi yield strengths, have required costly fabrication practices and lower than desired toughness.

1.2 Development of Bridge Steels with Improved Weldability and Toughness

In response to the need for steels with improved weldability and toughness, the Lehigh University ATLSS Center (Advanced Technology for Large Structural Systems) implemented a series of investigations** over a period of time to develop copper-nickel (Cu-Ni) steels with carbon contents reduced to less than 0.10 percent. This reduction in carbon content greatly improved toughness and also improved weldability by eliminating the need for preheat in most cases. However, increasing the copper content to the typical value of 1.00 percent resulted in the susceptibility of the steel to hot shortness during hot working. This problem was readily eliminated by the addition of nickel in an amount usually equal to ½ the copper content. This solution initiated the development of an ATLSS Cu-Ni structural steel that had a

** See Appendix

minimum yield strength of 100 ksi, designated as HPS 100W. HPS 100W has been fabricated into and erected at bridges in Nebraska and West Virginia. By adjusting the precipitation aging temperature, this Cu-Ni steel can be readily produced at minimum yield strengths of 70 to 100 ksi and thus meet many application requirements.

1.3 The Cost of Bridge Corrosion in the United States

The amount of money spent each year repairing and replacing corroded structures in the United States is startling. Studies have been performed to estimate the total corrosion cost in the US alone. The first study on the annual cost of corrosion in the United States was done by Battelle-NBS in 1975. They used "an economic input/output framework" and approximated the total cost of corrosion as $70 billion, which was equivalent to 4.2% of the gross national product (GNP) at that time. Twenty years later in the Transportation Equity Act for the 21st Century (TEA-21 Act), Congress ordered a new study. The Federal Highway Administration (FHWA) directed the second study, which was performed by teams from CC Technologies and NACE International. Brongers, a member of the CC Technologies team, estimated the cost of corrosion to be about $300 billion per year. This study[3] took a much more detailed approach by dividing the total corrosion cost into five industry divisions: infrastructure, utilities, transportation, production and manufacturing, and government. Brongers estimated each industry division's corrosion cost by taking its percentage of the gross domestic product (GDP) and multiplying it by the total GDP to get the corrosion cost for each division.

> "The following elements were included in these costs: cost of additional or more expensive material used to prevent corrosion damage, cost of labor attributed to corrosion management activities, cost of the equipment required because of corrosion-related activities, loss of revenue due to disruption in supply of product, cost of loss of reliability, and cost of lost capital due to corrosion deterioration"[3].

The industry division that is relevant to the focus of this paper was the infrastructure division because this includes the money spent on corrosion of highway bridges. It was estimated that 16.4% of the total annual corrosion cost was spent on the infrastructure division, which is equivalent to about $22.6 billion. Of the $22.6 billion, the amount spent on highway bridges was approximately $8.3 billion. This is the figure that FHWA is committed to reducing[3].

1.4 Past Development of Steels with Improved Corrosion Resistance

Researchers have been trying to develop an improved corrosion resistant steel for adverse environments for many years. During this period of time, new steel grades have been produced and more knowledge has been gained. High performance steels (HPS) were developed to offer bridge designers "high strength, corrosion resistance, fracture toughness and excellent weldability"[4].

JFE Steel located in Japan has developed two types of corrosion resistant weathering steel by adding nickel. They are referred to as JFE-ACL Type 1 and JFE-ACL Type 2 and their compositions are listed below. Type 1 has a basic composition of 1.5% Ni-0.3% Mo, and Type 2 has a basic composition 2.5% Ni and ultra-low C. In a comparison between Type 1 and Type 2, the lower Ni content of Type 1 reduces the cost but the addition of molybdenum increases corrosion

resistance. The high percentage of Ni in Type 2 is reported to enhance the corrosion resistance[5].

	C	Si	Mn	P	S	Cu	Ni	Mo
JFE-ACL 490 Type 1	0.07%	0.32%	0.71%	0.033%	0.002%	-	1.45%	0.32%
JFE-ACL 490 Type 2	0.02%	0.29%	0.92%	0.006%	0.005%	0.37%	2.68%	-

When selecting the chemical compositions for bridge steel grades, it is important to understand the impact of the elements involved. The carbon content in structural steels, usually between 0.15% and 0.20%, contributes the strength and hardenability to the steel, but reduces weldability and toughness. Corrosion resistance can be improved by adding copper, chromium, and phosphorous. These three elements produce "more tightly adherent oxide films when weathered," which reduces the need for a protective coating system[6]. Two disadvantages of adding phosphorous are that it decreases notch toughness and it is highly sensitive to cold- and hot-crackings during welding, resulting in a limitation on the steels plate thickness of under 16 mm (0.63 inches)[7]. According to Townsend, carbon, silicon, chromium, copper and nickel are all linked with corrosion resistance, and they are generally accepted with revised coefficients[8]. The proceeding observations are important considerations in the development of an improved corrosion resistant steel that will increase the life cycle of the steel.

To assist in increasing the life cycle of highway bridges, the FHWA contracted with ATLSS to develop an "improved corrosion resistant steel for highway bridge construction" with the following constraints. First, the steel had to be manufactured without significantly increasing its production cost above the cost

of the structural steels used for bridges today. An exception to this constraint would have been considered if and only if the life-cycle benefits of the new steel grade outweigh the higher initial cost. Second, the new steel had to "be capable of mass production within current capabilities of the steel industry in the United States"[1]. Third, the new steel had to fulfill the same mechanical properties listed in the ASTM A709 Specification. These properties include yield strength, tensile strength, ductility, and toughness. Fourth, the steel had to be readily welded by existing processes and had to be able to be machined and assembled by existing processes used for bridge construction. Finally, the new steel had to have increased atmospheric corrosion resistance for applications in areas in the United States where bridges are exposed to de-icing salts[1].

Although the writer participated in all aspects of the subject program, three specific aspects were assigned for thesis development. Two involved the application of multivariable regression analyses correlating multiple independent composition variables to various dependent variable experimental results. The specific programs were as follows:

1. Correlation between experimental compositions and mechanical properties—this information was necessary to ensure that the desired mechanical properties could be obtained when the experimental compositions departed significantly from the base composition shown in Table I.
2. Correlation between experimental compositions and accelerated corrosion data—this information is crucial to the selection of "improved corrosion

resistant" compositions for semifinal evaluation of "improved compositions" as described in the conclusions and recommendations for final "improved compositions".

3. Evaluation of the added cost to improve corrosion resistance—this information responds to the program requirement that "the improved steel have a cost similar to the corresponding A709 steels."

2. EXPERIMENTAL PROCEDURE

2.1 Melting and Rolling

This project originally consisted of 16 different chemical compositions for the new steel grade, which are labeled as Steel 1, Steel 2, etc (Table II). These compositions were created based on a two-level factorial program of the following variable elements: copper, silicon, chromium, and nickel. The 16 compositions were divided into four iterations by selecting the four compositions that covered each scenario of chromium-nickel or copper-nickel levels—low-low, high-low, low-high, and high-high. Every melt consisted of the first, second, and fourth composition from each iteration; therefore, low-high was left out each time.

Every iteration was created from a 300-pound (136 kg) heat performed by the United States Steel Technology Center in Munhall, PA. The heat produced three 100-pound (45.4 kg) ingots (3-inches thick by 8-inches wide by 14-inches long, including the hot top) of the selected experimental compositions. Each ingot was rolled to a 1-inch-thick (0.0254 m) plate and then the hot top and 6 inches (0.1524 m) of sound metal were removed for future use during mechanical-property tests.

The remaining steel plate was cut into four or five pieces which were reheated and rolled to 1/10-inch-thick (0.00254 m) sheets for future corrosion testing.

2.2 Heat Treatment

The 6-inch-long steel pieces were austenitized at 1650°F (900°C) and water-quenched. Samples were removed from the water-quenched pieces and Jominy end-quench hardenability, aging hardness, and mechanical-property tests were performed. Each iteration had 4 test pieces—as-quenched, aged at 1000°F (535°C), aged at 1100°F (595°C), and aged at 1200°F (650°C). The desirable minimum yield strength was 70 ksi (485 MPa).

2.3 Jominy Tests

Each steel had undergone four Jominy hardenability tests in accordance with ASTM A255 (austenitized at 1650°F and were end-quenched). The as-quenched samples were tested on both sides and their hardnesses were averaged. Then one specimen was reserved as as-quenched, one was aged at 1000°F, one at 1100°F, and another at 1200°F for one hour. The specimens were then ground to remove the previous hardness impressions, and retested in order to obtain the hardness values at different aging temperatures.

2.4 Mechanical-Property Tests

0.357 inch-diameter (0.00907 m) tension test and Charpy V-notch test specimens were removed from the quarter thickness location of the 1-inch-thick heat-treated plate. The tension specimens were tested for yield strength, tensile strength, elongation, and reduction of area. Charpy V-notch tests were conducted at

-40°F (-40°C), -80°F (-62.2°C), and -120°F (-84.4°C) to obtain the appropriate transition temperatures and related toughness data.

2.5 Weldability Tests

The carbon equivalent (CE) was calculated for each experimental steel by using the IIW formula: CE = C + Mn/6 + (Si + Cu + Ni)/15 + (Cr + Mo + V)/5. Steels with high CE values, which contained the most alloy content and were expected to demonstrate the best corrosion resistance, were plotted on a Graville Diagram (Figure 1). The Graville Diagram is divided into three zones. In Zone I, welds produced under most welding conditions are not susceptible to heat-affected-zone (HAZ) hydrogen-assisted cracking (HAC). In Zone II, welding requires some pre-heating and post-heating to prevent cracking, and in Zone III, the heat-affected-zone (HAZ) is extremely susceptible to cracking.

Implant tests were conducted to determine whether or not preheating was necessary for the experimental steels, particularly steels with low carbon content but very high CE values. These tests measured the susceptibility of the experimental steels to hydrogen-assisted cracking (HAC) when welded. A cylindrical threaded specimen was machined from the 1-inch thick plate. The specimen was inserted into a hole that was drilled into a 1-inch-thick steel test plate and a bead-on-plate weld was deposited over the hole. The welding was performed at room temperature with a low-hydrogen electrode by the shielded-metal-arc process at 200 amps, 8 inches/min (0.2032 m/min), corresponding to a heat input of 35 KJ/inch (1378 KJ/m). Once the welding was completed, the steel test plate was loaded with various test loads up to

and exceeding the experimental steel's yield stress. The highest stress that could be applied without fracture in 24 hours was the measure of the resistance of the steel to HAC upon welding without preheat using low-hydrogen electrodes.

2.6 Corrosion Tests

The resistance of the experimental steels to corrosion in highway bridges was measured by the mass loss (weight loss) of bare-metal samples exposed in a test chamber to an environment simulating the corrosive environment of highway bridges in the presence of deicing salt solutions. The effect of the corrosive environment was achieved by utilizing accelerated cyclic corrosion, which reduced the exposure time required to obtain significant corrosion. Experimental steel samples in previous studies have been exposed to existing corrosive environments such as the Moore Drive Bridge in Rochester, NY and the Kure Beach 25 meter lot (KB 25m). Both locations have a corrosivity category of C5, which is the highest category permitted by ASTM. The samples placed at these locations were removed at specific intervals and the evaluation of all results was performed according to ASTM standard testing guidelines. The data gathered from both sites was used to establish a correlation between accelerated corrosion in the chamber and time at Moore Drive Bridge.

Dr. Desmond Cook at Old Dominion University was responsible for conducting all the corrosion tests on 6" x 4" x 0.10" (0.1524m x 0.1016m x 0.00254m) specimens for steels 9, 10, 12, E, F, H, J, K, & M as well as benchmark steels A36, A588, and HPS100W. The benchmark steels were included as standards for comparative mass-loss data and for field correlation with known corrosion data

from Moore Drive Bridge in Rochester, NY. Fourteen coupons of each experimental steel were used to complete the accelerated corrosion testing. Of those 14 coupons, 3 were exposed in the corrosion test chamber at times of 1, 3, 5 and 10 weeks, and 2 were used as non-exposed mass-loss references in the chemical cleaning process.

The cleaning process utilized procedures specified by ASTM G-1 – Recommended practice for Preparing, Cleaning, and Evaluating Corrosion Test Specimens. Preparation included stamping each coupon with a code using a steel punch, removing any millscale by identically sandblasting each coupon with 170-325 μm (0.0067-0.0128 inches) glass beads at 45 psi (0.310 MPa), and degreasing each coupon with acetone. Each coupon was then weighed and measured to record the mass and area data.

The accelerated corrosion chamber contained 4 separate racks, which contained each experimental steel in triplicate; therefore a total of 36 coupons were positioned almost vertically in each rack. All racks were exposed to a modified SAE J2334, Laboratory Cyclic Corrosion Test, which ran on the 7 day/week protocol. The type of solution spray within the chamber was modified from a recommended 0.5% NaCl, 0.1% $CaCl_2$, and 0.075% $NaHCO_3$ to a 5 wt% NaCl solution without the $NaHCO_3$ buffer. The solution strength was increased in order to accurately simulate the intense weathering conditions observed in the US Snow Belt. In the chamber, jets sprayed the coupons with a fine mist of the 5 wt% NaCl solution for 15 minutes. The humidity in the chamber was then varied between 100% for 6 hours and 50% for

18 hours in order to simulate wet-dry cycles, which are critical for a steel to produce a protective patina.

The racks were removed from the chamber after 1, 3, 5, and 10 weeks exposure. Originally the fourth removal was scheduled for 7 weeks, but after reviewing the 1, 3, & 5 week data, it was decided to extend the exposure to 10 weeks. Coupons were photographed as they were removed from the chamber, to observe the colors, patterns, and differences between the steels. All coupons from the chamber were weighed for mass-gain data. Each experimental steel triplicate set and corresponding mass-loss references, which were not exposed, underwent identical rust stripping procedures as specified by ASTM G1, Chemical Cleaning Procedure C.3.5. The 3-, 5-, and 10-week exposures had a thicker, more adherent layer of rust, so they were lightly sandblasted prior to the chemical stripping. The coupons were weighed and photographed after each chemical stripping cycle. Once the coupons were stripped clean, the average corrosion rate was calculated for each coupon according to ASTM G1 designation and recorded into a master spreadsheet.

Mossbauer spectroscopy was also performed by Dr. Cook to identify the rusts which formed on the test samples. This additional analysis furnished valuable information on the chemical elements that provide the best resistance to corrosion. The results from the experimental steels were compared to the results from the benchmark steels which were sent to Dr. Cook. The benchmark steels are listed in Table I and they range from low-cost carbon steels known to be vulnerable to corrosive attack to higher-cost alloy steels with improved corrosion resistance.

Mossbauer spectroscopy is an analytical technique used on weathering steel to differentiate the corrosion products that make up its protective film. It is also used to distinguish the corrosion products that form in unfavorable conditions where the oxide coating is not protective to the steel. Mossbauer spectroscopy is able to identify "the nanophase components of the rust through the measurement of their magnetic relaxation at different temperatures." It is known as an "accurate, sensitive, non-destructive analytical technique" that is very popular because "it is able to calculate the fraction of each iron oxide present in the rust more accurately than X-ray diffraction"[9].

3. EXPERIMENTAL RESULTS AND DISCUSSION

3.1 Iteration 1 – Steels 9, 10 & 12

3.1.1 Melting and Rolling

The first melt produced three 100-pound ingots of experimental composition Steels 9, 10, and 12, from Table II.

3.1.2 Jominy Tests

Figures 2, 3, and 4 illustrate the Jominy curves for steels 9, 10, and 12. The hardness test results ranged from 26 to 33 H_{RC}, which correspond to a range of tensile strengths of about 124 to 154 ksi (855 to 1060 MPa). The results of Steel 9, Figure 2 show that the as-quenched material is strengthened by tempering at all temperatures, except 1200°F at distances less than 12/16 inch (0.01905 m) and 1100°F at distances less than 7/16 inch (0.01111 m). The strengthening is a result of the competition between softening due to tempering of the martensite and

strengthening due to precipitation of the copper-rich particles. The greatest strengthening occurred at 1000°F because of the three temperatures softening was at a minimum. At 1200°F, softening prevailed because the precipitates grew larger and less effective. The effect of temper aging for each of the steels is portrayed in Figures 2, 3, and 4, respectively.

Each figure shows that the hardness values for the as-quenched and the three aged specimens for each steel were all above the desired approximate yield strength maximum of 80 ksi (552 MPa). The Jominy curves were relatively flat for Steels 9, 10, and 12, which indicated that the hardenability was very high. These results suggested the reduction of the carbide forming elements because they produce excessive hardenability.

3.1.3 Mechanical-Property Tests

Due to the undesirable high hardness for Steels 9, 10, and 12, the mechanical-property tests were not performed.

3.1.4 Weldability-Tests

The Cu-Ni experimental steels plotted on the Graville diagram fall into Zone I, as seen in Figure 1. The figure indicates benchmark Steel A1010 and experimental Steel 12 fall beyond the Zone I CE limit; therefore, the Graville Diagram suggest these steels will probably require preheat.

3.2 Iteration 2 – Steels J, K, & M

Based on the results from experimental Steels 9, 10, and 12, it was decided to reduce the hardenability of the steels by eliminating the carbide formers—chromium,

molybdenum, and vanadium—and increasing the ferrite formers—manganese, silicon, copper, and nickel. The range of the carbon content was varied from [0.04%, 0.06%] to [0.03%, 0.06%], and the range of the silicon content from [0.75%, 1.25%] to [0.75%, 2.00%]. These changes can be seen in Tables II and III.

Figure 5 shows the linear relationship between carbon content and the hardness of 99.9% martensite down to 0.10% carbon. Linear extrapolation suggests that the carbon content must be lower than 0.06% to avoid excessive hardness. Use of the ferrite formers rather than the carbide formers was expected to increase resistance to corrosion without resulting in the formation of martensite at undesirable hardness levels.

3.2.1 Melting and Rolling

The second melt produced three 100-pound ingots of experimental composition Steels J, K and M, from Table III. The resultant compositions can be seen in Table IV.

3.2.2 Jominy Tests

Figure 6 shows the Jominy curves for Steel J. The as-quenched specimen hardness at the quenched end begins at 29 HRc and drops steeply to 12.5 HRc around 10/16-inch (0.01588 m) from the quenched end. The curve slowly approaches 10 HRc at 32/16-inch (0.0508 m). These test results indicate that a tensile strength of about 90 ksi (621 MPa) can be expected even in heavy sections of Steel J. The curves for the temper-aged material lie lower than the as-quenched curve toward the quenched end due to the result of temper softening of the existing

hard martensite. As the distance from the quenched end increases, the precipitation strengthening outweighs the temper softening, causing the temper-aged curves to lie above the as-quenched curve. A tensile strength of about 107 ksi (738 MPa) can be expected for Steel J when tempered at 1000°F, and a range of 92 to 98 ksi (634 to 655 MPa) can be expected when tempered at 1100°F or 1200°F.

A similar trend exists for Steels K & M, which can be seen in Figures 7 & 8. The Jominy curves for Steel K have shifted upward indicating higher hardenability and yield strength values. This upward shift is due to the increase in nickel content from 0.75% to 2.00%. Steel M's Jominy curves lie even higher than Steel K, which indicate a further increase in hardenability. This increase is a result of the increase of copper content from 1.25% to 2.00%.

3.2.3 Mechanical-Property Tests

The tensile and Charpy V-notch tests were performed on Steels J, K, & M quenched and temper-aged at 1100°F and 1200°F. The yield strength ranged from 80 to 108 ksi (552 to 738 MPa) seen in Table V, which indicates that the desired minimum yield strength of 70 to 80 ksi (483 to 552 MPa) can be readily achieved by these experimental steels. The tensile strength ranged from 92 to 115 ksi (634 to 793 MPa) also seen in Table V. Steels J, K, & M showed excellent ductility, measured by elongation and reduction of area. The Charpy V-notch energy absorptions and transition temperatures indicate the safe use of these steels in fracture-critical applications in the lowest temperature zones specified in ASTM A709.

3.2.4 Weldability Tests

Implant tests were performed on Steel M, which was selected because it has a high CE value of 0.61 and it showed promising corrosion resistance. The tests resulted in failures that occurred at stresses below the yield stress. The results indicated that this steel may require preheat for welding. Zone I in the Graville Diagram (Figure 1) may be misleading because Steel M has a low carbon content (0.06%) but may require preheating at the fairly high CE value (0.61). Based on these results, steels with low carbon contents and CE values greater than 0.60 shown on the Graville Diagram may require preheat despite lying in Zone I.

3.3 Iteration 3 – Steels E, F, & H

The next iteration selection from Table III was Steels E, F, and H. These were chosen with the intent to observe the effect of carbon and silicon on hardness, strength, toughness, ductility, weldability, and corrosion resistance. The carbon content between Iteration 2 & 3 decreased from 0.06% to 0.03%, and the silicon content increased from 0.75% to 2.00%.

3.3.1 Melting and Rolling

The second melt produced three 100-pound ingots of experimental composition Steels E, F and H, from Table III. The resultant compositions can be seen in Table IV.

3.3.2 Jominy Tests

The Jominy curves for Steels E, F, and H are shown in Figures 9, 10 & 11. Yield strengths from 95 to 130 ksi (655 to 896 MPa) can be achieved in these three

experimental steels. Figure 9 reveals the highest hardness (23 HRc) occurs at 1000°F and the lowest (14 HRc) in the as-quenched specimen. Temper-aging resulted in the expected behavior: as temperature increases, temper softening increases and net strengthening decreases.

The Jominy curves for Steel F (Figure 10) lie higher than the curves for Steel E. Once again, this is a consequence of increasing the nickel content from 0.75% to 2.00%. The as-quenched specimen is harder than all aged specimens through 4/16-inch (0.00635 m) from the quenched end. Then it rapidly drops in hardness and flattens out around 22 HRc with the curves for specimens aged at 1100°F and 1200°F. The specimen temper-aged at 1000°F displayed a uniformly higher hardness beyond 5/16-inch (0.00794 m); the result again of the age-strengthening exceeding the temper-softening.

As seen in Figure 11, the as-quenched and the 1000°F curves for Steel H nearly coincide at plate thicknesses beyond 1-inch. The 1100°F and 1200°F curves nearly coincide at plate thicknesses beyond 1-inch as well, and were consistently softer than the as-quenched and 1000°F specimens.

3.3.3 Mechanical-Property Tests

There was an insufficient amount of steel available to perform the mechanical-property tests on Steels E, F, and H.

3.3.4 Weldability Tests

Implant tests were not performed on Steels E, F, or H.

3.4 Iteration 4 – Steels A, B, & D

Our next iteration selection from Table III consisted of Steels A, B, & D. These steels were chosen to focus on the effect of carbon by comparing the various test results with Steels J, K, & M. The Jominy results were also compared with Steels E, F, & H to study the affect of silicon on hardenability. The carbon content between Iterations 2 & 4 decreased from 0.06% to 0.03%, and the silicon content between Iterations 3 & 4 decreased from 2.00% to 0.75%.

3.4.1 Melting and Rolling

The melt produced three 100-pound ingots of experimental composition Steels A, B, and D from Table III. The resultant compositions can be seen in Table IV.

3.4.2 Jominy Tests

Figure 12 illustrates the hardenability for Steel A. The specimen results for temper-aged at 1000°F are consistently higher than the other curves and resulted in the highest hardness value of about 19 HRc. As seen in previous Jominy curves, temper softening increased with temperature and tempered strengthening decreased with temperature. Steel B Jominy curves are plotted in Figure 13. The hardenability increased from Steel A to B in keeping with the nickel content. The as-quenched curve and the temper-aged at 1200°F curve behaved similarly after 8/16-inch (0.01270 m) from the quenched end. As shown in Figure 14, Steel D produced the highest hardness values in the as-quenched and temper-aged at 1000°F specimens. The corresponding tensile strengths range from 100 to 115 ksi (689 to 793 MPa).

The upward shift in the curves from Steel B to Steel D probably is a result of the increase in copper content from 1.25% to 2.00%.

3.4.3 Mechanical-Property Tests

The tensile and Charpy V-notch tests were performed on Steels A, B, and D quenched and temper-aged at 1000°F, 1100°F, and 1200°F. The yield strength ranged from 73 to 101 ksi (503 to 696 MPa) in Table VI, which indicates that the desired minimum yield strength of 70 to 80 ksi (483 to 552 MPa) can be achieved by the experimental steels. The tensile strength ranged from 82 to 112 ksi (565 to 772 MPa) in Table VI. Steels A, B, & D showed excellent ductility, measured by elongation and reduction of area. The Charpy V-notch energy absorptions and transition temperatures were extraordinarily good and indicate the safe application of these steels in fracture-critical applications in the lowest temperature zones specified in ASTM A709.

3.4.4 Weldability Tests

Implant tests were not performed on Steels A, B, or D.

3.5 Corrosion Tests

The results of the accelerated corrosion chamber test for the experimental and benchmark steels are shown in Table VII. The table lists the total average thickness-loss for 1-, 3-, 5-, and 10-weeks for each pair of exposed coupons. Based on the results, the most corrosion resistant steel is experimental Steel 12. Steel 12 has the least thickness-loss after 10 weeks of 361 microns. All the experimental steels

performed better than the benchmark steels after being exposed in the accelerated corrosion test chamber.

The results are also illustrated in Figure 15 for a visual interpretation of the corrosion performance. The ideal result is a linear trend that begins to plateau, which would indicate the presence of a protection offered by the steel. Looking at Figure 15, Steel 12 demonstrates the desirable trend because the line begins to flatten after 5-weeks exposure. Steel E also demonstrates the desired trend, but it lies higher on the chart because its thickness-loss is greater than Steel 12. Additionally, M and H performed well in the corrosion chamber. Both of these steels were showing promising outcomes at 3- and 5-weeks, but neither one began to plateau after 10-weeks. These results suggest that Steels M and H did not produce a protective coating like Steel 12 and Steel E.

3.6 Cost Analysis

The total cost for each experimental steel was calculated by adding the individual cost per pound for each element—copper, nickel, silicon, chromium—to the total base composition cost of $0.42/lb. The base cost was established from the cost of $0.42/lb charged by U.S. Steel for producing HPS100W steel in its final heat-treated form that was used to fabricate and erect the highway bridge over I80 outside Omaha, Nebraska as seen in Illustration 1.

The current costs for copper, nickel, silicon, and chromium are as follows:

	Copper	Nickel	Silicon	Chromium
Cost/lb	$ 3.10	$ 14.17	$ 1.50	$ 1.96

Nickel is obviously the most expensive element used in the experimental steel compositions; therefore, it is very desirable to limit the addition of nickel. The amount of copper should also be limited due to its higher cost compared to silicon and chromium. The total cost of each experimental steel is listed in Table VIII.

4. MULTIVARIABLE REGRESSION ANALYSIS

The objective of the multivariable regression analysis was to look for meaningful relationships between the experimental steel compositions and their mechanical-property and corrosion performance in order to predict an ideal composition for future use in highway bridges. The software used to conduct the multivariable regression analysis was StatGraphics 5.0. The analysis consisted of comparing one dependent variable versus multiple independent variables. The dependent variables used in this analysis were tensile strength, yield strength, Charpy V-notch energy absorption, hardness, and thickness-loss by corrosion. The independent variables consisted of the experimental composition elements – carbon, silicon, copper, nickel, and chromium.

4.1 Mechanical-Property Analysis

The intent of the statistical analysis of the mechanical-property data for Steels A, B, D, and J, K, M (Table IX) was to establish correlations between hardness, strength, fracture toughness, and the experimental chemical compositions. The relations of the mechanical properties to the composition of the experimental steels and their statistical reliability are listed in Table X. Silicon was left out of this study because it does not vary among Steels A, B, D and J, K, M.

4.1.1 Composition – Yield Strength Analysis

The statistical results indicate that the yield strength can be estimated from chemical composition and tempering temperature with good reliability. When yield strength is predicted from chemical composition, the derived equation, shown in Table X-A, explains 92.4% of the variability. The relation between the predicted and observed values for yield strength is portrayed in Figure 16.

4.1.2 Composition – Tensile Strength Analysis

The effect of chemical composition and tempering temperature on tensile strength is illustrated in Table X-B. The correlation coefficient of 93% implies a good correlation. The equation indicates that temper-aging temperature decreases tensile strength as it increases. The equation also indicates that carbon, copper, and nickel all increase the tensile strength. Figure 17 shows the relationship between predicting the tensile strength from the observed data equation.

4.1.3 Composition – Toughness Analysis

The equation for predicting the Charpy V-notch energy absorbed at -40°F from the composition and tempering temperature is listed in Table X-C. Note that all the added composition elements decreased the energy absorption and the tempering temperature increased it. The effect of increasing the tempering temperature was expected to increase the toughness but reduce the strength. The effect was the greatest for carbon, less for nickel, and the least for copper. The plot of predicted values from the combined-data equation is shown in Figure 18.

4.2 Hardenability Analysis

The intent of the statistical analysis on the hardness data for 1-inch- and 2-inch- (0.0508m) thick plates of the experimental Steels A, B, D, E, F, H, J, K, & M (Table XI) was to identify the effect of each chemical element on the hardenability of the steels. The relationships and their statistical reliability are listed in Table XII.

4.2.1 Composition – Hardness As Quenched

The statistical relationships for 1-inch- and 2-inch-thick plate are listed in Table XII-A. Both equations have a very good correlation indicated by the R values which are above 99%. The largest positive coefficient in both equations is associated with carbon. This indicates that carbon has the largest impact on the hardenability of the experimental steels at the as-quenched state.

4.2.2 Composition – Hardness at 1000°F

The chemical composition and hardness relationships for 1-inch- and 2-inch-thick plate are listed in Table XII-B. The accuracy of using the observed data equation to predict the hardness value is very good because the correlation coefficients are around 98%. All four elements—carbon, silicon, copper, and nickel—increase the hardenability as shown by their positive coefficients.

4.2.3 Composition – Hardness at 1100°F

The correlation coefficient for the 1-inch-thick plate data equals 98.4%, and for the 2-inch-thick plate data equals 96.2%, Table XII-C. These statistical factors denote the very good reliability of estimating hardness from the chemical composition at 1100°F.

4.2.4 Composition – Hardness at 1200°F

The outputs of this analysis are listed in Table XII-D. Both equations explain over 97% of the variability.

4.3 Thickness-Loss Data Analysis

The intent of the multivariable regression analysis on the 10-week thickness-loss data was to establish a relationship between chemical compositions and corrosion performance that could be used to predict an ideal steel composition. The data used to perform this analysis is listed in Table XIII. The equation, shown in Table XIV, relates the thickness-loss values after 10-week exposure in the accelerated corrosion chamber and the silicon, copper, nickel, and chromium content. The correlation coefficient of 85.1% indicates a good correlation between the composition and thickness-loss. Figure 19 illustrates the accuracy of using the equation to predict thickness-loss from chemical composition.

Copper has the largest coefficient in the equation, which indicates that it has the largest impact on the corrosion performance of the steel. The higher the copper content, the lower the thickness-loss. This result is not surprising because copper is always included in the compositions for A709 steels. It is a major contributor in A36 and A588. Nickel has the lowest coefficient, and it is a positive value; therefore, reducing the nickel content will improve the corrosion performance and decrease the cost of the steel. The silicon and chromium coefficients indicate that both these elements impact the thickness-loss, so more tests on experimental compositions with various levels of silicon and chromium content are encouraged.

5. CONCLUSIONS

On the basis of the preceding results and discussion, the following important conclusions can be drawn:

1. Multivariable regression analyses have been developed for predicting the effect of chemical composition on the mechanical properties of experimental steels.
    a. Carbon has the largest coefficient in all the statistical relationships, indicating that it has the greatest affect on the mechanical properties.
    b. Copper and silicon have similar, low coefficients in the statistical equations, which imply they both have minimal effects on the mechanical property results.
2. Multivariable regression analyses have been developed for predicting the effect of chemical composition on the accelerated corrosion performance of experimental steels.
    a. Nickel has a positive coefficient in the statistical equation, which suggests reducing the nickel content in order to decrease the thickness-loss value and the total cost of the steel.
    b. Carbon has the largest negative coefficient in the statistical equation, which indicates increasing the carbon content will improve the corrosion resistance of the steel.
3. Equations have been developed for predicting the total cost of commercial production of experimental compositions from the base Cu-Ni steel.

These conclusions in combination constitute the methodology for continuing the development of an improved corrosion resistant steel for highway bridge construction and recommending continued experimental approaches. Thus the projects assigned to the subject thesis have been successfully completed.

6. RECOMMENDATIONS FOR FUTURE WORK

1. Complete evaluation of Steels U, V, and W to determine the effect of silicon and chromium additions to the base Cu-Ni steel.
2. Produce 500-lb (226.8 kg) heat(s) of final improved composition steel(s).
   a. Produce 500-lb heat of chemical composition based on observations of previous results.
      i. Roll plates to thicknesses of 1-, ½-, and ¼-inch and air cool.
      ii. Conduct mechanical-property tests on air-cooled plates.
      iii. Conduct mechanical-property tests on quenched and aged plates.
      iv. Conduct implant tests on selected plates to establish weldability.
      v. Conduct accelerated corrosion tests and ambient exposure tests.
   b. Produce 500-lb heat of chemical composition based on multivariable regression analysis relating chemical composition to selected dependent variables.
      - Repeat items i-v listed above.
3. Produce commercial heat of optimum composition from 2 above by the basic oxygen or electric furnace process.
   a. Obtain FHWA approval for production and funding of commercial heat.

b. Negotiate with states for approval and location of two Interstate bridges — one to be in the area of heavy salt use and one in the area of moderate salt use.

c. Melt a provision heat to supply plates for the two highway bridges.

   i. Include up-to-date metallurgical ladle treatment to control composition and temperature.

   ii. Pour slabs of required sizes using continuous-cast variable mold.

   iii. Roll slabs to plate and treat to required properties.

d. Conduct detailed mechanical-property and weldability tests to confirm data.

e. Conduct accelerated corrosion tests and ambient exposure tests in various locations.

4. Obtain information on design, engineering, fabrication, erection, and projected maintenance costs from cooperating states, involved bridge fabricators, and FHWA.

   a. Compare results on projected life-cycle cost basis for improved steel with corresponding information for current ASTM A709 steels (presumably A588/A852).

Benchmark Steels													
	C	**Mn**	**P**	**S**	**Si**	**Cu**	**Ni**	**Cr**	**Mo**	**V**	**Cb**	**Al**	**CE**
A36	0.055	0.93	0.013	0.009	0.20	0.30	0.17	0.20	0.05	0.002	---	0.026	0.30
A588-1	0.120	1.14	0.014	0.012	0.36	0.31	0.30	0.52	0.003	0.037	---	0.056	0.49
A588-2	0.110	0.97	0.011	0.015	0.37	0.27	0.24	0.52	0.09	0.036	---	---	0.46
A852	0.091	1.26	0.017	0.008	0.37	0.30	0.30	0.56	0.10	0.060	---	0.016	0.51
HPS 100W	0.056	1.00	0.006	0.003	0.27	1.00	0.75	0.51	0.49	0.060	0.003	0.032	0.57
A1010	0.030	1.50	0.040	0.005	1.00	---	1.50	12.00	---	---	---	---	2.85

Table I – Chemical Compositions of Benchmark Steels, %

Base Composition												
C	Mn	P	S	Si	Cu	Ni	Cr	Mo	V	Cb	Al	CE
0.04	1.45	0.015	0.003	0.75	1.20	0.75	0.50	0.50	0.06	0.020	0.030	0.67

Variable Elements

C: 0.04 and 0.06
Si: 0.75 and 1.25
Cr: 0.50 and 4.00
Ni: 0.75 and 2.00

Proposed Compositions					
Steel	C	Si	Cr	Ni	CE
1	0.04	0.75	0.50	0.75	0.67
2	0.04	0.75	0.50	2.00	0.75
3	0.04	0.75	4.00	0.75	1.37
4	0.04	0.75	4.00	2.00	1.45
5	0.04	1.25	0.50	0.75	0.70
6	0.04	1.25	0.50	2.00	0.79
7	0.04	1.25	4.00	0.75	1.4
8	0.04	1.25	4.00	2.00	1.49
9	0.06	0.75	0.50	0.75	0.69
10	0.06	0.75	0.50	2.00	0.77
11	0.06	0.75	4.00	0.75	1.39
12	0.06	0.75	4.00	2.00	1.47
13	0.06	1.25	0.50	0.75	0.72
14	0.06	1.25	0.50	2.00	0.81
15	0.06	1.25	4.00	0.75	1.42
16	0.06	1.25	4.00	2.00	1.51

Table II – Two Level Factorial Program to Optimize Composition of Corrosion-Resistant Steels Base Composition and Proposed Compositions of Experimental Steels 1-16, %

Base Composition												
C	Mn	P	S	Si	Cu	Ni	Cr	Mo	V	Cb	Al	CE
0.03	1.45	0.015	0.003	0.75	1.25	0.75	LAP	LAP	LAP	0.020	0.030	0.45

Variable Elements

C: 0.03 and 0.06
Si: 0.75 and 2.00
Cu: 1.25 and 2.00
Ni: 0.75 and 2.00

Proposed Compositions					
Steel	C	Si	Cu	Ni	CE
A	0.03	0.75	1.25	0.75	0.45
B	0.03	0.75	1.25	2.00	0.53
C	0.03	0.75	2.00	0.75	0.50
D	0.03	0.75	2.00	2.00	0.58
E	0.03	2.00	1.25	0.75	0.53
F	0.03	2.00	1.25	2.00	0.62
G	0.03	2.00	2.00	0.75	0.58
H	0.03	2.00	2.00	2.00	0.67
J	0.06	0.75	1.25	0.75	0.48
K	0.06	0.75	1.25	2.00	0.56
L	0.06	0.75	2.00	0.75	0.53
M	0.06	0.75	2.00	2.00	0.61
N	0.06	2.00	1.25	0.75	0.56
R	0.06	2.00	1.25	2.00	0.65
S	0.06	2.00	2.00	0.75	0.61
T	0.06	2.00	2.00	2.00	0.70

Table III – Two Level Factorial Program to Optimize Composition of Corrosion-Resistant Steels Base Composition and Proposed Compositions of Experimental Steels A-T, %

Steel	C	Mn	P	S	Si	Cu	Ni	Cr	Mo	V	Cb	Al	CE
J	0.070	1.49	0.017	0.004	0.76	1.24	0.76	0.006	0.001	0.003	0.02	0.033	0.50
K	0.071	1.45	0.017	0.004	0.76	1.26	1.99	0.005	0.001	0.004	0.02	0.029	0.58
M	0.075	1.45	0.017	0.004	0.75	1.96	1.97	0.005	0.001	0.004	0.02	0.028	0.63
E	0.032	1.49	0.013	0.003	2.08	1.30	0.74	0.005	0.001	0.002	0.02	0.037	0.56
F	0.028	1.46	0.013	0.002	2.00	1.28	1.98	0.005	0.001	0.002	0.02	0.034	0.62
H	0.036	1.45	0.013	0.003	2.01	1.89	1.96	0.005	0.001	0.002	0.02	0.037	0.67
A	0.023	1.43	0.015	0.002	0.75	1.31	0.73	0.006	0.004	0.002	0.02	0.037	0.45
B	0.024	1.40	0.014	0.002	0.75	1.30	1.93	0.006	0.004	0.002	0.02	0.029	0.53
D	0.024	1.40	0.014	0.020	0.75	2.04	1.92	0.006	0.004	0.002	0.02	0.027	0.57

Table IV – Actual Compositions of Steels J, K, M, E, F, H, & A, B, D, %

Steel J

C	Mn	P	S	Si	Cu	Ni	Cr	Mo	V	Cb	Al
0.070	1.49	0.017	0.004	0.76	1.24	0.76	0.006	0.001	0.003	0.018	0.033

		Tensile Properties					Hard	Charpy V-Notch Transition Temperature					Charpy V-Notch Energy				
		YS	TS	EL	RA	YS/TS	HRc	20 ft-lb	35 ft-lb	60 ft-lb	15 mils	50% FAT	70	0	-40	-80	-120
Laboratory Water Quench Plus																	
Temper @ 1100	JAC	86	98	28	76	0.88	15.2	---	---	---	---	-55	---	---	140	105	90
Temper @ 1200	JAE	80	92	30	76	0.87	13.3	---	---	---	---	-90	---	---	205	160	135

Steel K

C	Mn	P	S	Si	Cu	Ni	Cr	Mo	V	Cb	Al
0.071	1.45	0.017	0.004	0.76	1.26	1.99	0.005	0.001	0.004	0.018	0.029

		Tensile Properties					Hard	Charpy V-Notch Transition Temperature					Charpy V-Notch Energy				
		YS	TS	EL	RA	YS/TS	HRc	20 ft-lb	35 ft-lb	60 ft-lb	15 mils	50% FAT	70	0	-40	-80	-120
Laboratory Water Quench Plus																	
Temper @ 1100	KAC	108	111	28	72	0.93	18.6	---	---	---	---	>-40	---	---	105	85	40
Temper @ 1200	KAE	92	103	29	74	0.89	16.6	---	---	---	---	-100	---	---	145	130	105

Steel M

C	Mn	P	S	Si	Cu	Ni	Cr	Mo	V	Cb	Al
0.075	1.45	0.017	0.004	0.75	1.96	1.97	0.005	0.001	0.004	0.018	0.028

		Tensile Properties					Hard	Charpy V-Notch Transition Temperature					Charpy V-Notch Energy				
		YS	TS	EL	RA	YS/TS	HRc	20 ft-lb	35 ft-lb	60 ft-lb	15 mils	50% FAT	70	0	-40	-80	-120
Laboratory Water Quench Plus																	
Temper @ 1100	MAC	107	115	26	72	0.93	19.7	---	---	---	---	>-40	---	---	75	60	35
Temper @ 1200	MAE	98	107	28	74	0.92	17.8	---	---	---	---	-80	---	---	145	125	100

Table V – Mechanical Property Test Results of Steels J, K, & M*

*Average of Duplicate Test Specimens

Steel A

C	Mn	P	S	Si	Cu	Ni	Cr	Mo	V	Cb	Al
0.023	1.43	0.015	0.002	0.75	1.31	0.73	0.006	0.004	0.002	0.02	0.037

		Tensile Properties					Hard	Charpy V-Notch Transition Temperature					Charpy V-Notch Energy				
		YS	TS	EL	RA	YS/TS	HRc	20 ft-lb	35 ft-lb	60 ft-lb	15 mils	50% FAT	70	0	-40	-80	-120
Laboratory Water Quench Plus																	
Temper @ 1000	AAA	88	102	23	80	0.86	19.2	<-120	<-120	<-120	<-120	-100	---	---	120	110	75
Temper @ 1100	AAC	76	88	22	81	0.86	14.6	<-120	<-120	<-120	<-120	<-120	---	---	240	210	150
Temper @ 1200	AAE	73	82	29	83	0.89	11.2	<-120	<-120	<-120	<-120	<-120	---	---	240	240	240

Steel B

C	Mn	P	S	Si	Cu	Ni	Cr	Mo	V	Cb	Al
0.024	1.40	0.014	0.002	0.75	1.30	1.93	0.006	0.004	0.002	0.02	0.029

		Tensile Properties					Hard	Charpy V-Notch Transition Temperature					Charpy V-Notch Energy				
		YS	TS	EL	RA	YS/TS	HRc	20 ft-lb	35 ft-lb	60 ft-lb	15 mils	50% FAT	70	0	-40	-80	-120
Laboratory Water Quench Plus																	
Temper @ 1000	BAA	93	106	26	76	0.88	20.3	-120	-110	-100	-110	>-40	---	---	85	70	20
Temper @ 1100	BAC	83	96	29	78	0.86	15.4	<-120	<-120	<-120	<-120	-120	---	---	180	150	130
Temper @ 1200	BAE	79	91	29	80	0.87	13.1	<-120	<-120	<-120	<-120	-120	---	---	240	240	130

Steel D

C	Mn	P	S	Si	Cu	Ni	Cr	Mo	V	Cb	Al
0.024	1.40	0.014	0.020	0.75	2.04	1.92	0.006	0.004	0.002	0.02	0.027

		Tensile Properties					Hard	Charpy V-Notch Transition Temperature					Charpy V-Notch Energy				
		YS	TS	EL	RA	YS/TS	HRc	20 ft-lb	35 ft-lb	60 ft-lb	15 mils	50% FAT	70	0	-40	-80	-120
Laboratory Water Quench Plus																	
Temper @ 1000	DAA	101	112	25	71	0.90	22.9	-110	-60	-40	-100	-30	---	---	65	25	10
Temper @ 1100	DAC	82	92	28	76	0.89	19.1	<-120	-110	-90	<-120	-60	---	---	120	100	40
Temper @ 1200	DAE	91	99	28	78	0.92	16.3	<-120	<-120	<-120	<-120	<-120	---	---	240	160	130

Table VI – Mechanical Property Test Results of Steels A, B, & D*

*Average of Duplicate Test Specimens

Average Total Thickness Loss, microns				
Steel	**1 week**	**3 weeks**	**5 weeks**	**10 weeks**
9	58.160	207.315	360.819	837.003
10	49.797	184.999	326.576	928.655
12	39.234	144.897	262.450	361.155
J	53.705	177.791	343.315	634.799
K	52.586	160.619	286.713	606.140
M	50.465	167.240	264.670	561.453
M w/ millscale	66.510	195.563	315.969	622.515
E	53.054	171.529	307.597	553.932
F	52.752	159.420	282.782	593.416
H	55.436	153.099	281.653	556.460
A36	68.913	249.010	439.623	916.917
100W	59.050	210.542	442.595	913.124
A588	67.755	260.212	462.686	931.316

Table VII – Results of Accelerated Corrosion Tests

Steel	Si	Cu	Ni	Cr	Cost Addition	Total Cost
9	0.75	1.20	0.75	0.50	$ 0.16	$ 0.58
10	0.75	1.20	2.00	0.50	$ 0.34	$ 0.76
12	0.75	1.20	2.00	4.00	$ 0.41	$ 0.83
A	0.75	1.25	0.75	0.006	$ 0.16	$ 0.58
B	0.75	1.25	2.00	0.006	$ 0.33	$ 0.75
C	0.75	2.00	0.75	0.006	$ 0.18	$ 0.60
D	0.75	2.00	2.00	0.006	$ 0.36	$ 0.78
E	2.00	1.25	0.75	0.005	$ 0.18	$ 0.60
F	2.00	1.25	2.00	0.005	$ 0.35	$ 0.77
G	2.00	2.00	0.75	0.005	$ 0.20	$ 0.62
H	2.00	2.00	2.00	0.005	$ 0.38	$ 0.80
J	0.75	1.25	0.75	0.006	$ 0.16	$ 0.58
K	0.75	1.25	2.00	0.005	$ 0.33	$ 0.75
L	0.75	2.00	0.75	0.005	$ 0.18	$ 0.60
M	0.75	2.00	2.00	0.005	$ 0.36	$ 0.78
N	2.00	1.25	0.75	0.006	$ 0.18	$ 0.60
R	2.00	1.25	2.00	0.006	$ 0.35	$ 0.77
S	2.00	2.00	0.75	0.006	$ 0.20	$ 0.62
T	2.00	2.00	2.00	0.006	$ 0.38	$ 0.80

Table VIII – Total Cost of Experimental Steels 9, 10, 12 & A-T

Steel	Temper-Aged at, °F	Yield Strength, ksi	Tensile Strength, ksi	Charpy V-notch Energy at -40°F, ft-lb	Carbon, %	Silicon, %	Copper, %	Nickel, %
J	1100	86	98	140	0.06	0.75	1.25	0.75
	1200	80	92	205	0.06	0.75	1.25	0.75
K	1100	102	111	105	0.06	0.75	1.25	2.00
	1200	92	103	145	0.06	0.75	1.25	2.00
M	1100	107	115	75	0.06	0.75	2.00	2.00
	1200	98	107	145	0.06	0.75	2.00	2.00
A	1000	88	102	120	0.03	0.75	1.25	0.75
	1100	76	88	240	0.03	0.75	1.25	0.75
	1200	73	82	240	0.03	0.75	1.25	0.75
B	1000	93	106	85	0.03	0.75	1.25	2.00
	1100	83	96	180	0.03	0.75	1.25	2.00
	1200	79	91	240	0.03	0.75	1.25	2.00
D	1000	101	112	65	0.03	0.75	2.00	2.00
	1100	82	92	120	0.03	0.75	2.00	2.00
	1200	91	99	240	0.03	0.75	2.00	2.00

Table IX – Mechanical Property Data for Steels J, K, M, & A, B, D

Table X-A – Composition – Yield Strength Relationship

$YS = 124.50 - 0.069Temp\ (°F) + 416.30C + 8.00Cu + 7.36Ni$
$R^2 = 85.4\%, \Sigma = 4.60$

Table X-B – Composition – Tensile Strength Relationship

$TS = 152.56 - 0.079Temp\ (°F) + 394.07C + 4.80Cu + 7.20Ni$
$R^2 = 86.4\%, \Sigma = 4.17$

Table X-C – Composition – Toughness Relationship

$E_{-40°F} = -456.20 + 0.77Temp\ (°F) - 2333.33C - 29.33Cu - 30.40Ni$
$R^2 = 91.5\%, \Sigma = 21.99$

Table X– Statistical Relationships between Composition and Mechanical Properties for Steels J, K, M & A, B, D

1-inch plate	Quenched	1000°F	1100°F	1200°F	Carbon	Silicon	Copper	Nickel
E	15.3	22.9	18.9	17.1	0.03	2.00	1.25	0.75
F	24.9	26.2	23.7	24.5	0.03	2.00	1.25	2.00
H	28.2	28.2	26.6	26.0	0.03	2.00	2.00	2.00
J	17.5	19.9	18.5	15.2	0.06	0.75	1.25	0.75
K	24.8	22.5	21.6	19.7	0.06	0.75	1.25	2.00
M	27.8	25.4	23.1	20.9	0.06	0.75	2.00	2.00
A	10.9	20.4	14.6	13.0	0.03	0.75	1.25	0.75
B	17.5	21.0	16.7	15.5	0.03	0.75	1.25	2.00
D	21.0	24.2	20.0	18.2	0.03	0.75	2.00	2.00

2-inch plate	Quenched	1000°F	1100°F	1200°F	Carbon	Silicon	Copper	Nickel
E	13.1	22.7	18.0	16.0	0.03	2.00	1.25	0.75
F	21.7	26.1	20.9	21.9	0.03	2.00	1.25	2.00
H	26.6	27.0	24.1	23.2	0.03	2.00	2.00	2.00
J	11.6	19.8	15.0	12.2	0.06	0.75	1.25	0.75
K	17.8	21.3	18.8	15.6	0.06	0.75	1.25	2.00
M	22.2	23.6	19.0	17.4	0.06	0.75	2.00	2.00
A	8.3	19.2	14.7	11.1	0.03	0.75	1.25	0.75
B	13.3	20.5	15.0	13.0	0.03	0.75	1.25	2.00
D	20.0	23.2	18.8	16.0	0.03	0.75	2.00	2.00

Table XI – 1-inch and 2-inch Plate Hardness Data at Various Aging Temperatures for Steels A, B, D, E, F, H, & J, K, M

Table XII-A – Composition – Hardness at As Quenched Relationship

For 1-inch plate:
HR_c (As Quenched) $= -10.69 + 230.00C + 5.07Si + 4.36Cu + 6.27Ni$
$R^2 = 98.8\%$, $\Sigma = 0.91$

For 2-inch plate:
HR_c (As Quenched) $= -12.45 + 111.11C + 5.28Si + 7.11Cu + 5.28Cu$
$R^2 = 98.4\%$, $\Sigma = 1.08$

Table XII-B – Composition – Hardness at 1000F Relationship

For 1-inch plate:
HR_c (1000°F) $= 10.65 + 24.44C + 3.12Si + 3.60Cu + 1.73Ni$
$R^2 = 96.6\%$, $\Sigma = 0.73$

For 2-inch plate:
HR_c (1000°F) $= 11.24 + 20.00C + 3.44Si + 2.62Cu + 1.65Ni$
$R^2 = 97.4\%$, $\Sigma = 0.62$

Table XII-C – Composition – Hardness at 1100F Relationship

For 1-inch plate:
HR_c (1100°F) $= 0.20 + 132.22C + 4.77Si + 3.42Cu + 2.67Ni$
$R^2 = 96.8\%$, $\Sigma = 0.94$

For 2-inch plate:
HR_c (1100°F) $= 4.08 + 47.78C + 3.87Si + 3.20Cu + 1.87Ni$
$R^2 = 92.6\%$, $\Sigma = 1.18$

Table XII-D – Composition – Hardness at 1200F Relationship

For 1-inch plate:
HR_c (1200°F) $= -1.33 + 101.11C + 5.57Si + 2.40Cu + 3.84Ni$
$R^2 = 95.2\%$, $\Sigma = 1.34$

For 2-inch plate:
HR_c (1200°F) $= -1.33 + 56.67C + 5.60Si + 2.71Cu + 2.99Ni$
$R^2 = 96.8\%$, $\Sigma = 1.03$

Table XII – Statistical Relationships between Composition and Hardness at Various Aging Temperatures for Steels A, B, D, E, F, H, & J, K, M

Steel	10 weeks	C	Si	Cu	Ni	Cr
9	837.003	0.067	0.76	1.16	0.74	0.51
10	928.655	0.070	0.76	1.13	1.92	0.50
12	361.155	0.072	0.76	1.08	1.83	3.82
J	634.799	0.070	0.76	1.24	0.76	0.006
K	606.140	0.071	0.76	1.26	1.99	0.005
M	561.453	0.075	0.75	1.96	1.97	0.005
M w/ millscale	622.515	0.075	0.75	1.96	1.97	0.005
E	553.932	0.032	2.08	1.30	0.74	0.005
F	593.416	0.028	2.00	1.28	1.98	0.005
H	556.460	0.036	2.01	1.89	1.96	0.005
A36	916.917	0.055	0.20	0.30	0.17	0.20
100W	913.124	0.056	0.27	1.00	0.75	0.51
A588	931.316	0.120	0.36	0.31	0.30	0.52

Table XIII – Thickness Loss Data for Steels 9, 10, 12, E, F, H, & J, K, M

Table XIV – Composition – Thickness-Loss Relationship

Thickness-Loss = 1078.63 - 116.17Si - 197.07Cu + 8.634Ni - 99.34Cr

$R^2 = 72.5\%$, $\Sigma = 120.673$

Table XIV – Statistical Relationship between Compositions and Thickness Loss Data for Steels 9, 10, 12, E, F, H, & J, K, M

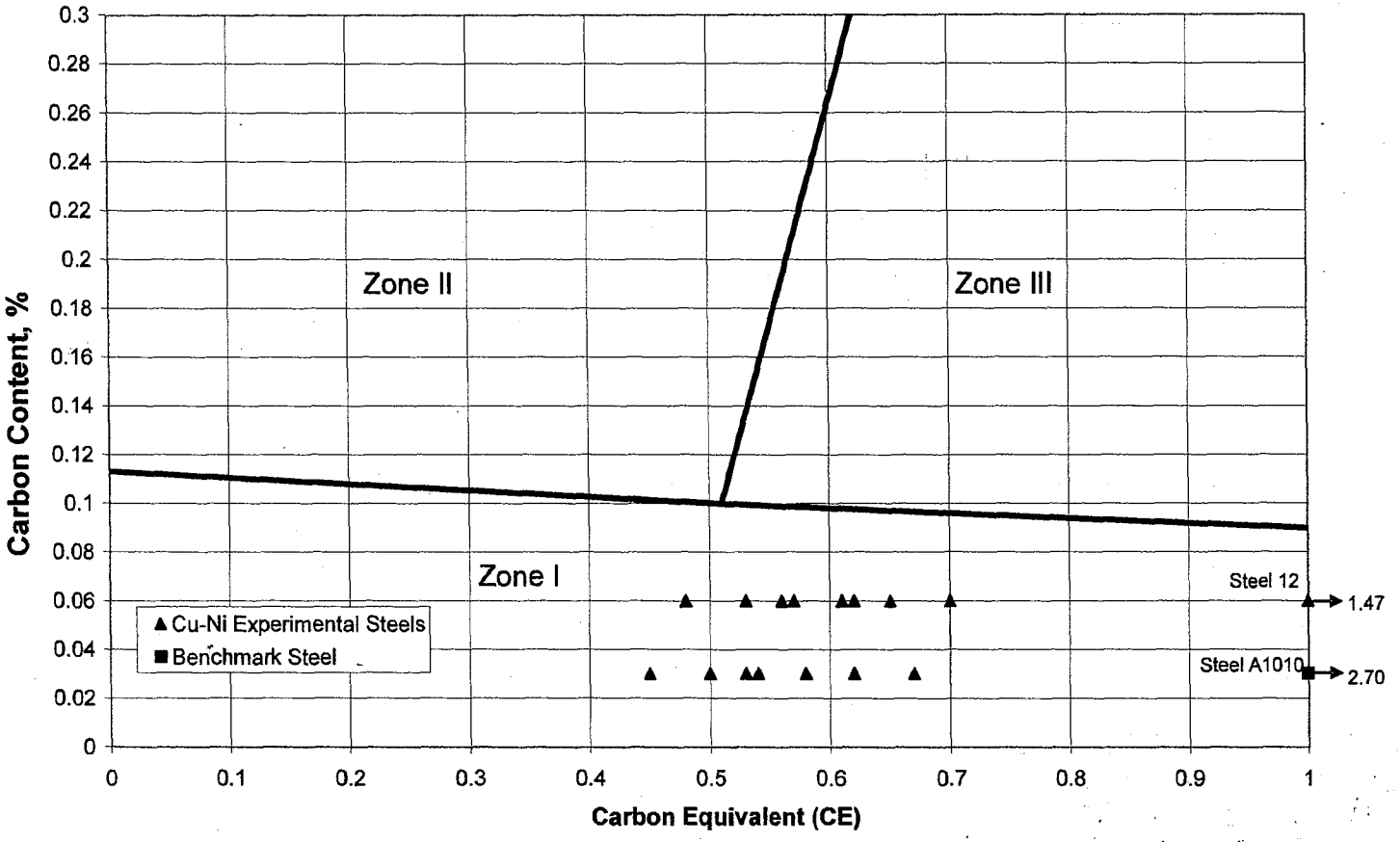

Figure 1 – Graville Diagram

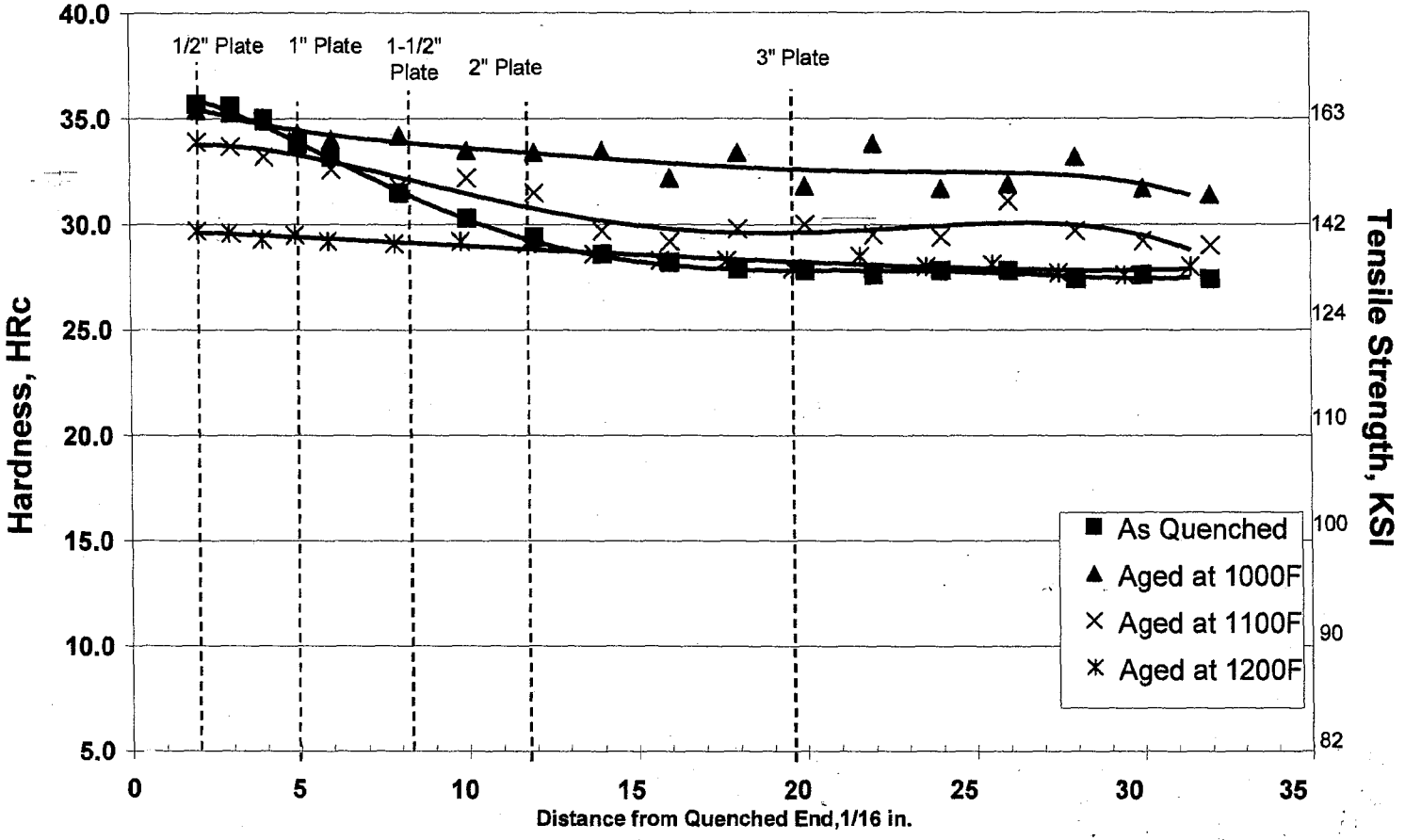

Figure 2 – Jominy Hardenability of Steel 9

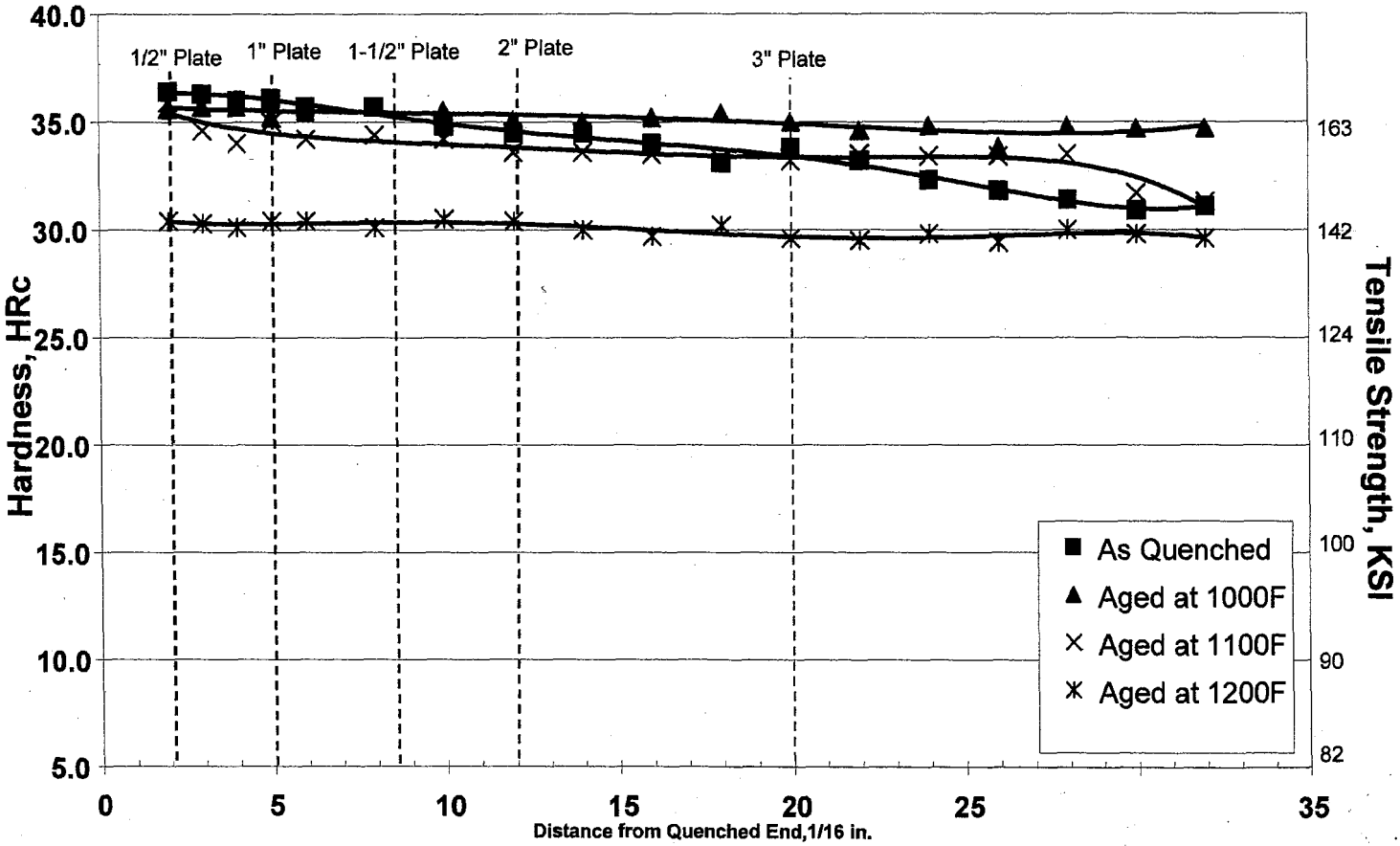

Figure 3 – Jominy Hardenability of Steel 10

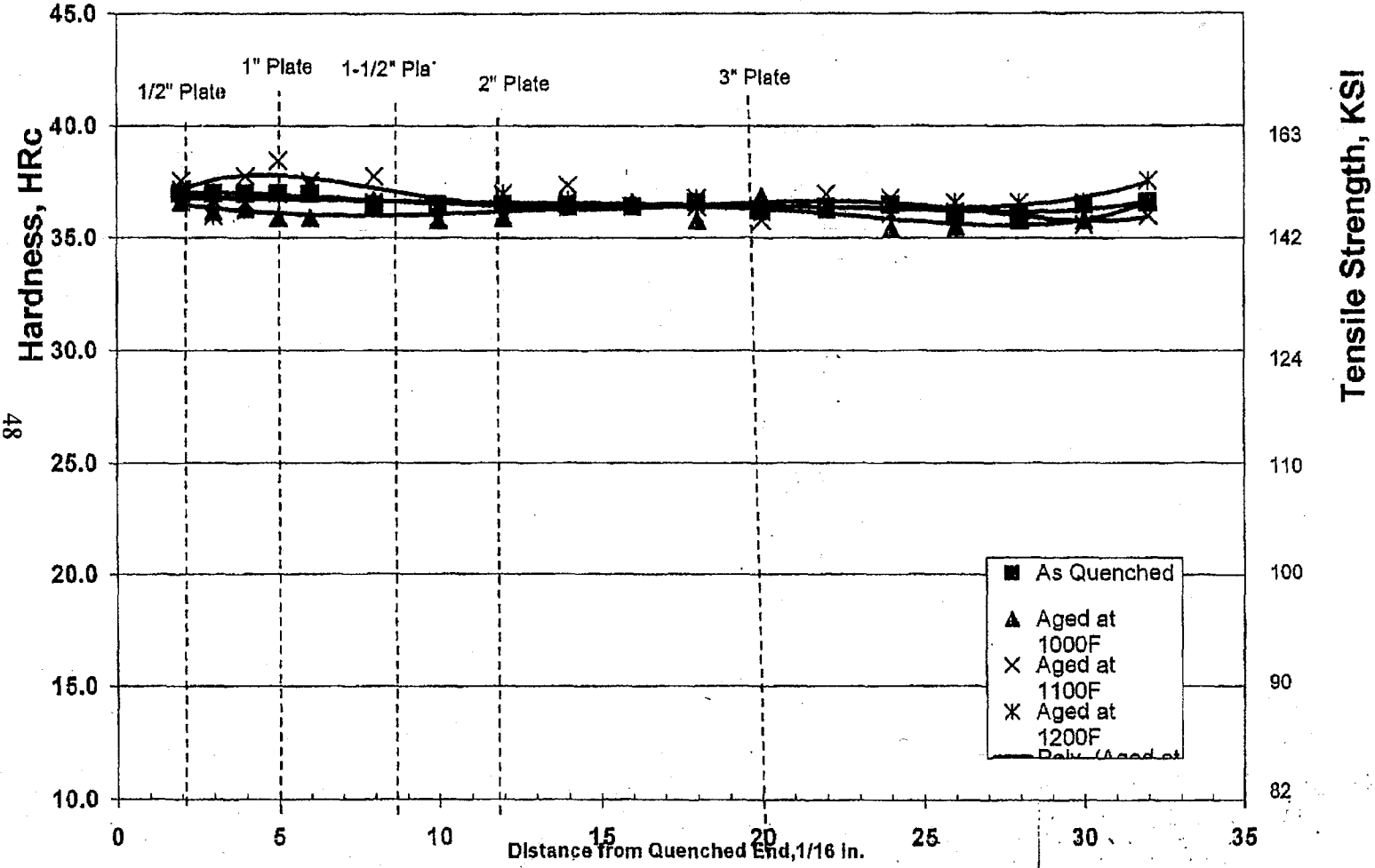

Figure 4 – Jominy Hardenability of Steel 12

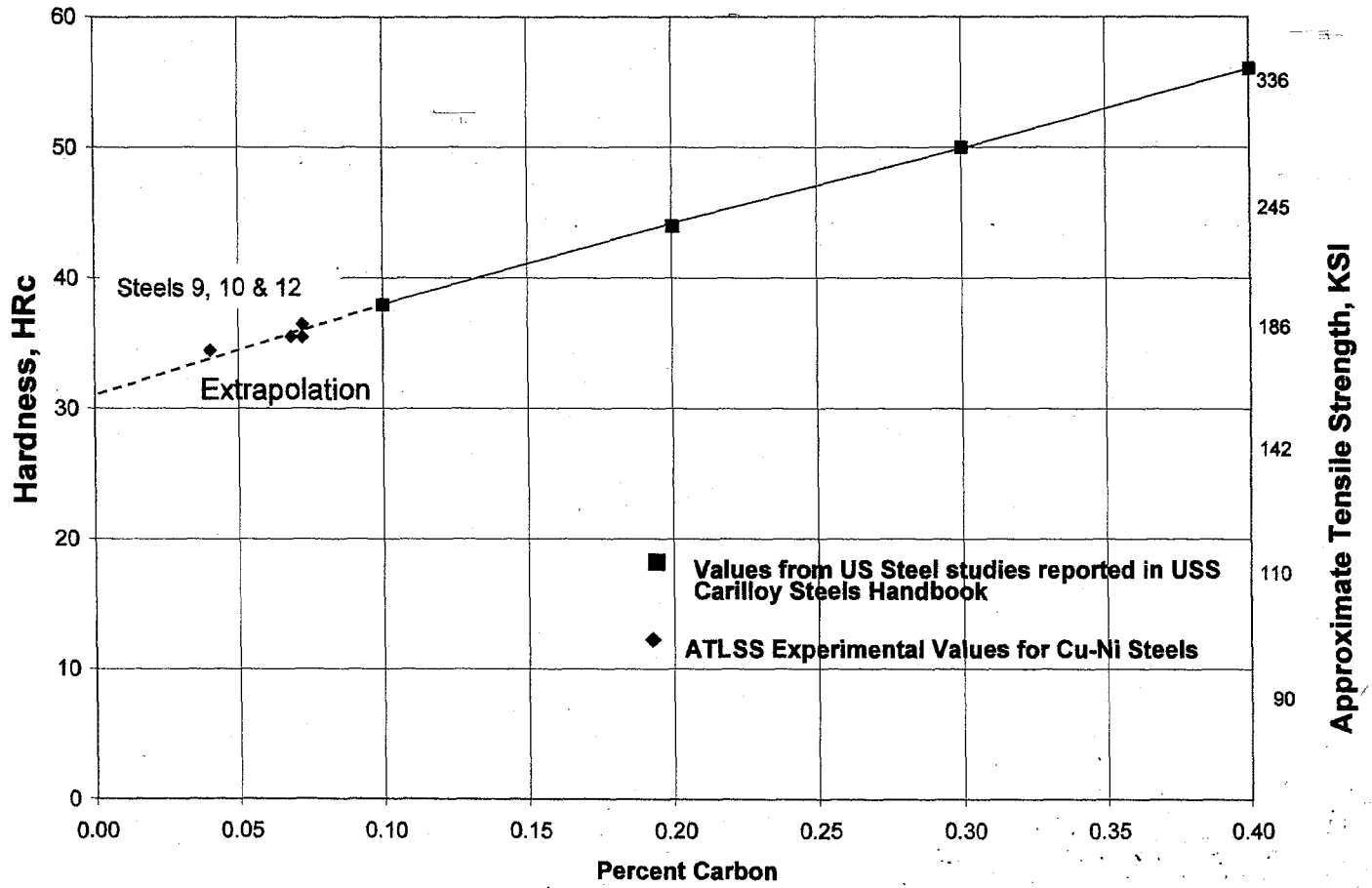

Figure 5 – Hardness of 99.9% Martensite at Various Carbon Contents

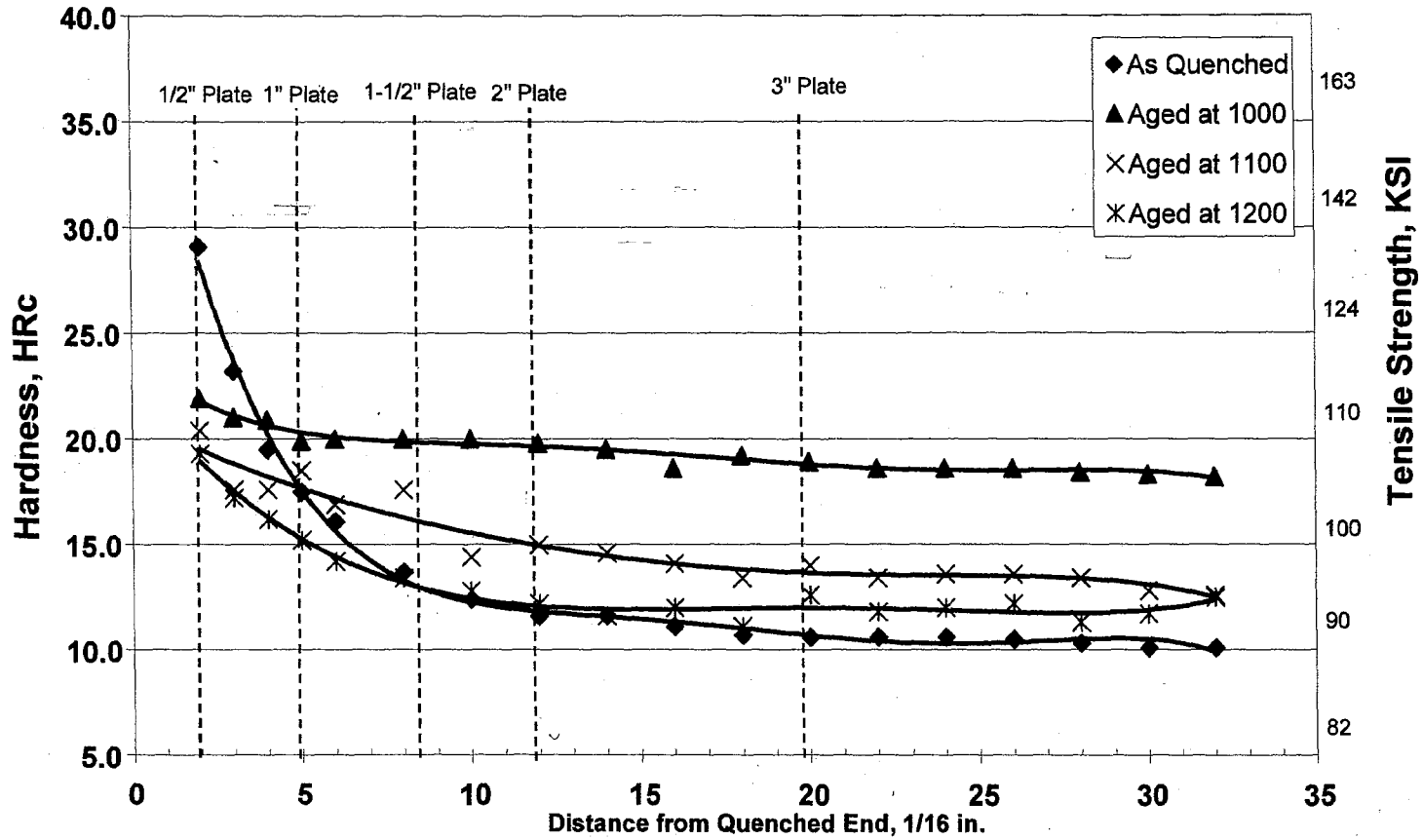

Figure 6 – Jominy Hardenability of Steel J

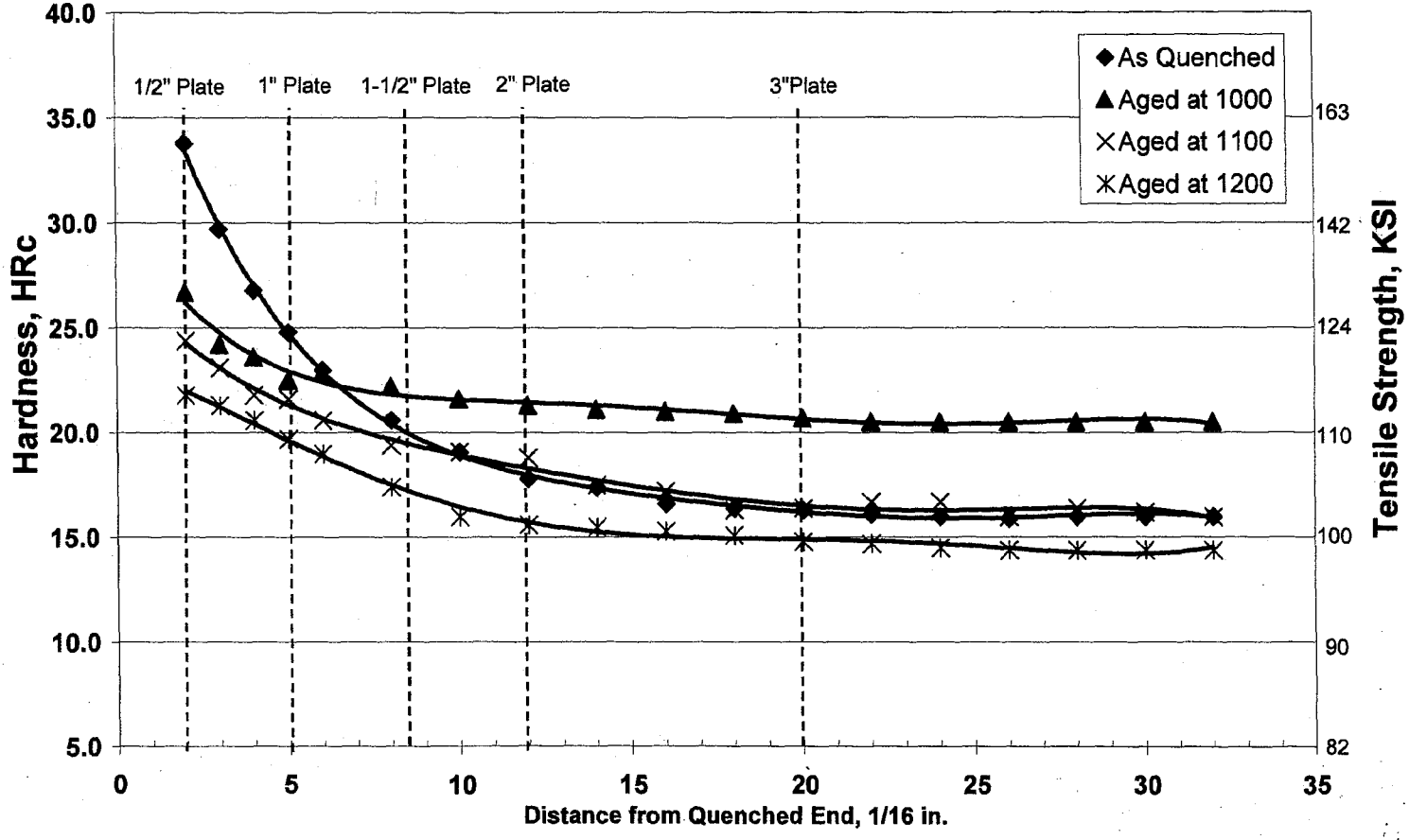

Figure 7 – Jominy Hardenability of Steel K

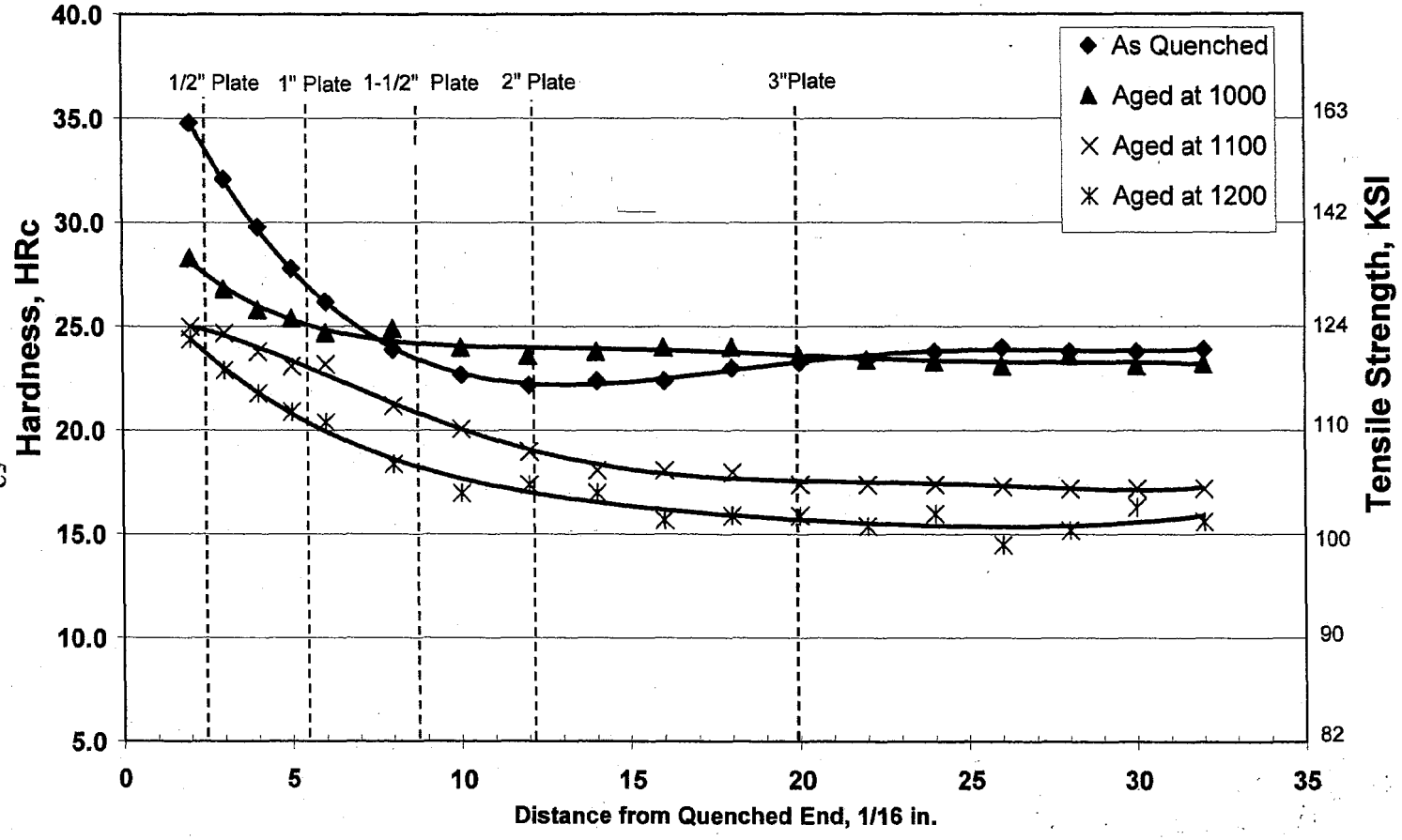

Figure 8 – Jominy Hardenability of Steel M

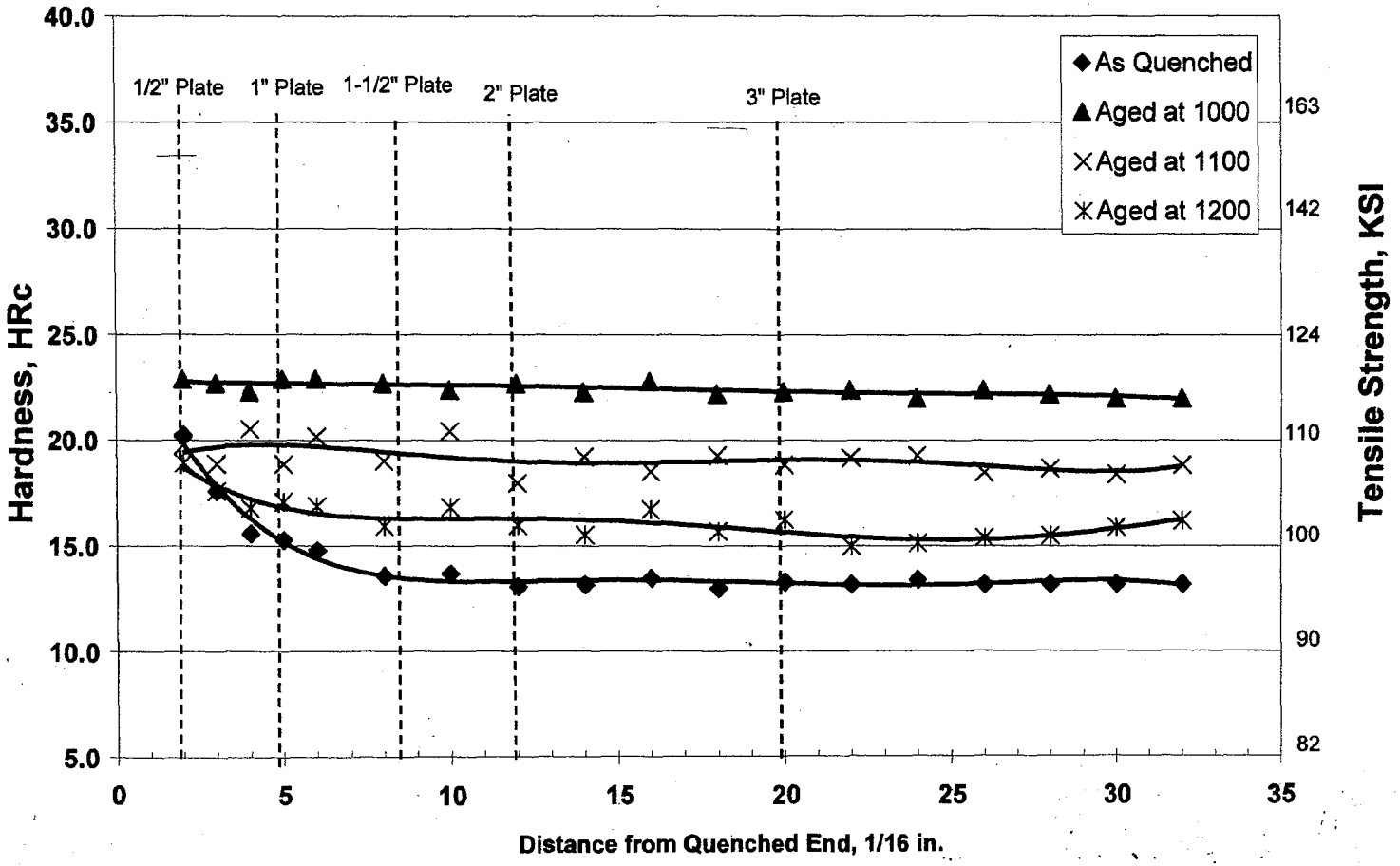

Figure 9 – Jominy Hardenability of Steel E

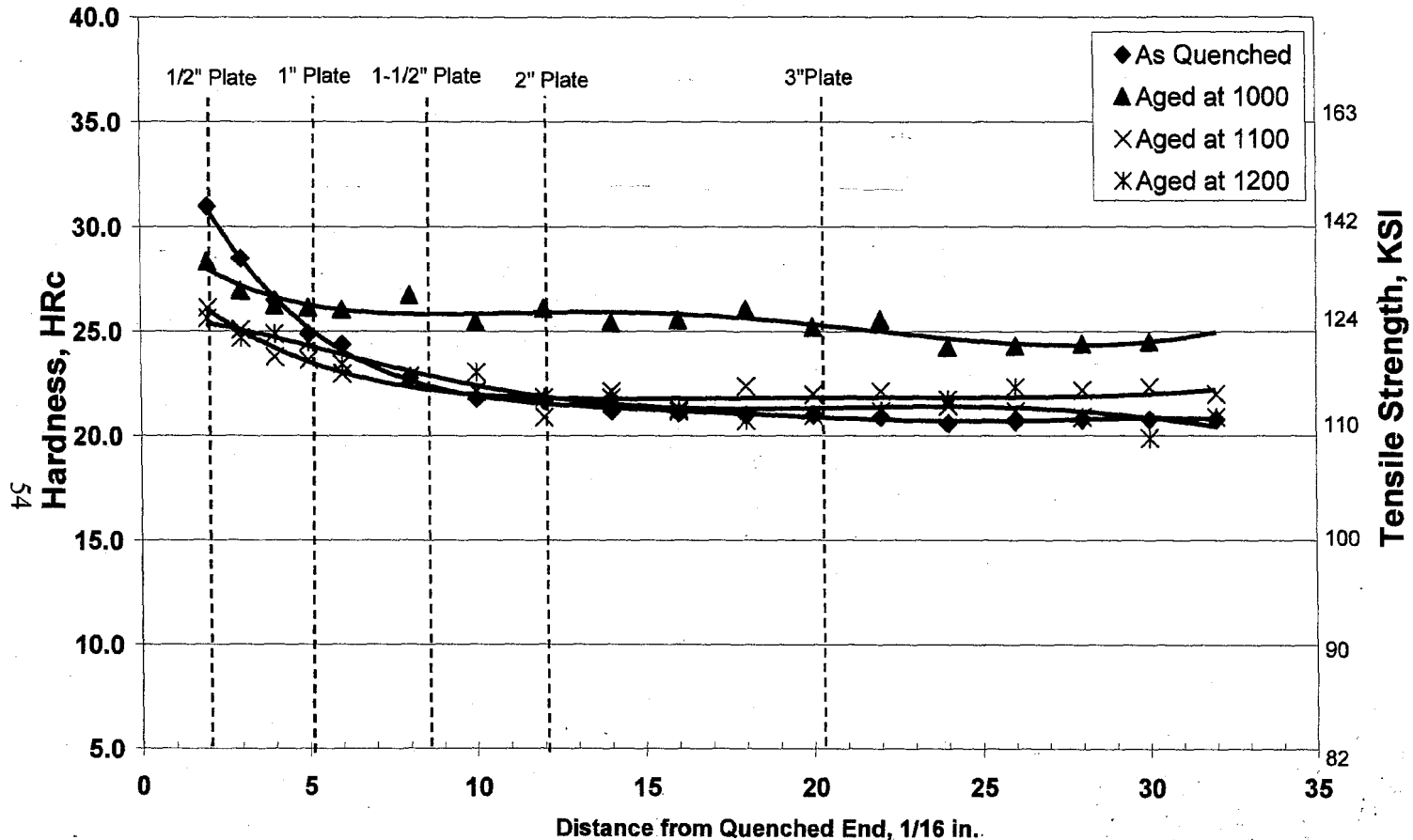

Figure 10 – Jominy Hardenability of Steel F

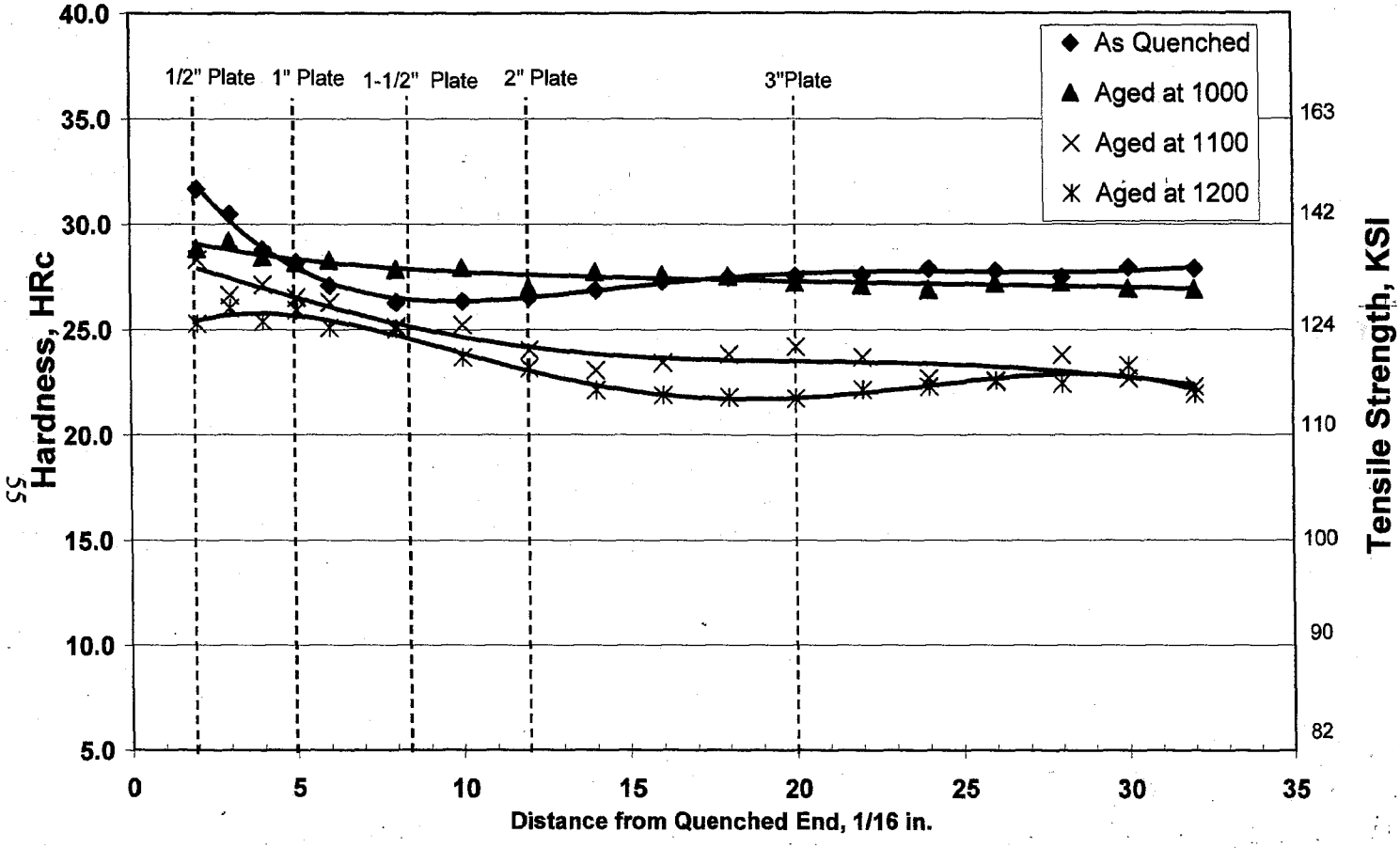

Figure 11 – Jominy Hardenability of Steel H

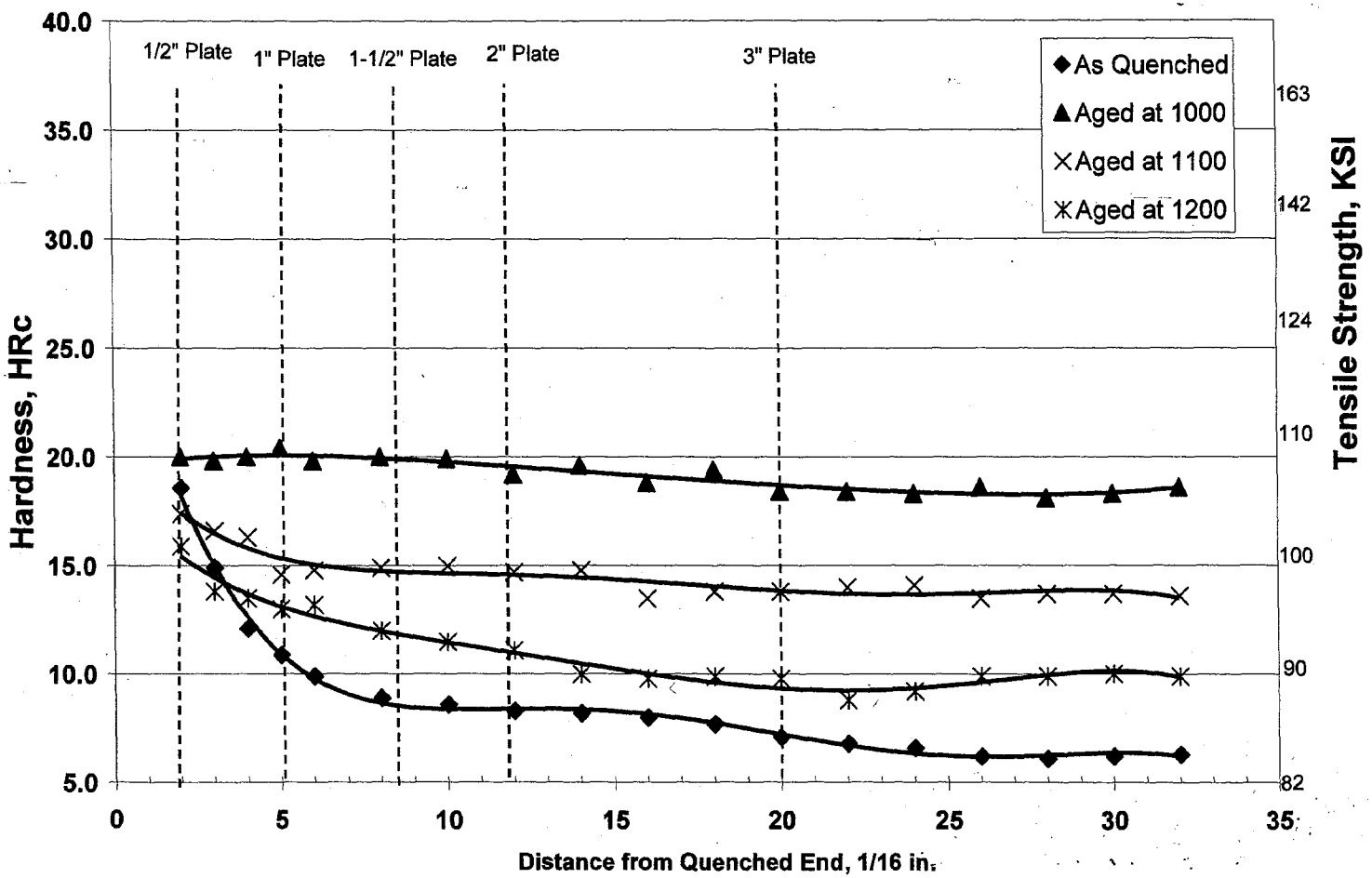

Figure 12 – Jominy Hardenability of Steel A

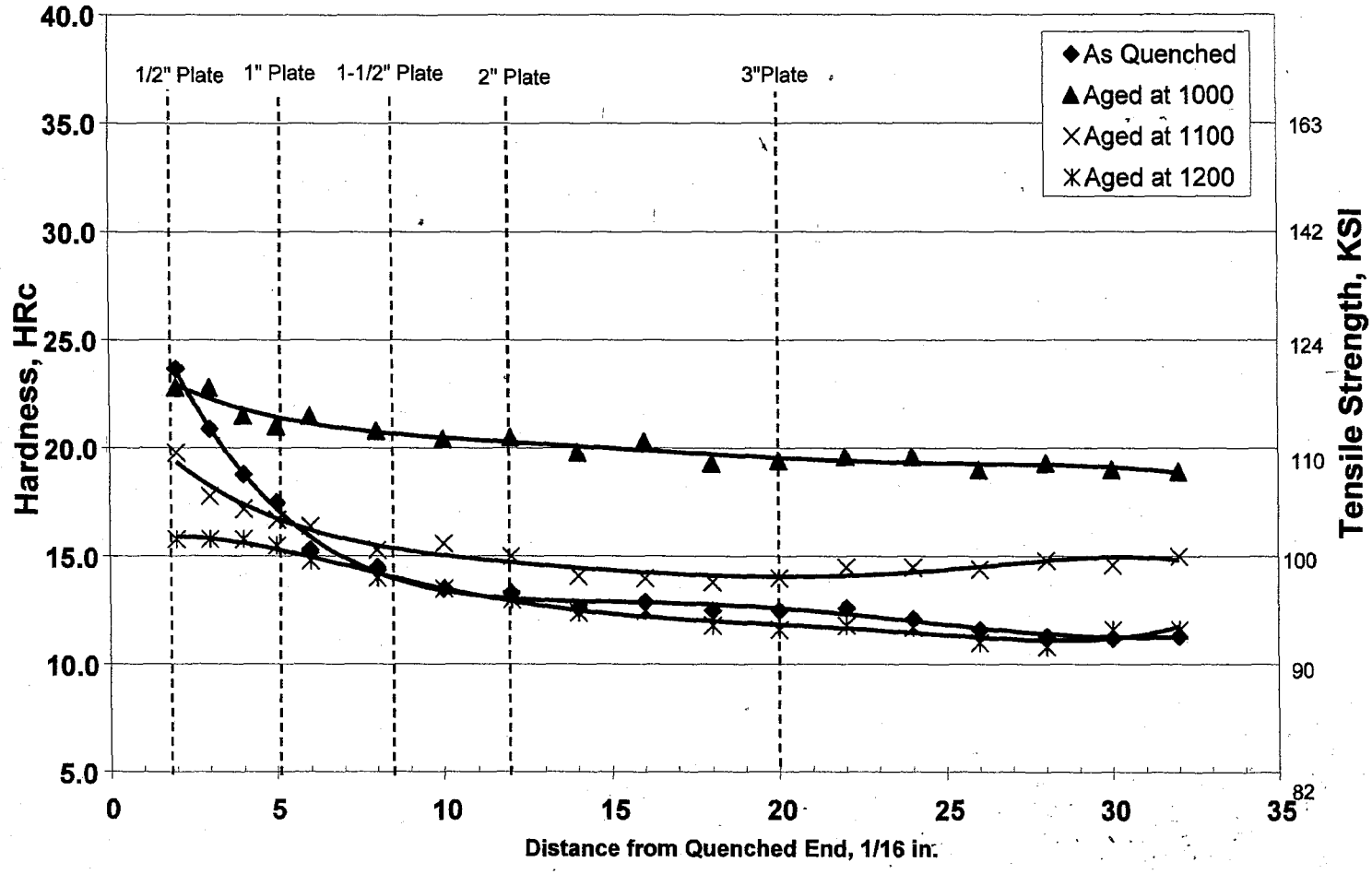

Figure 13 – Jominy Hardenability of Steel B

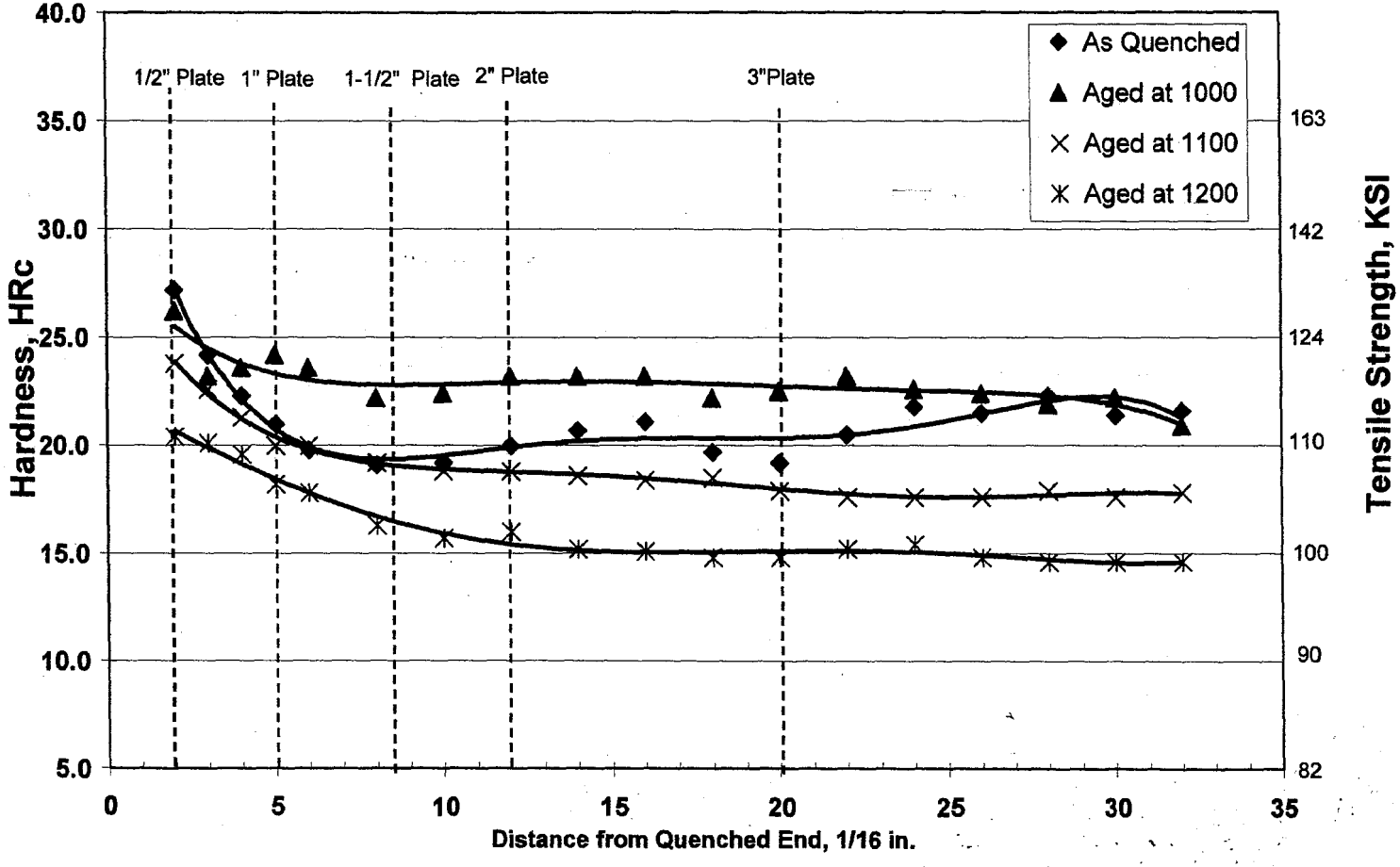

Figure 14 – Jominy Hardenability of Steel D

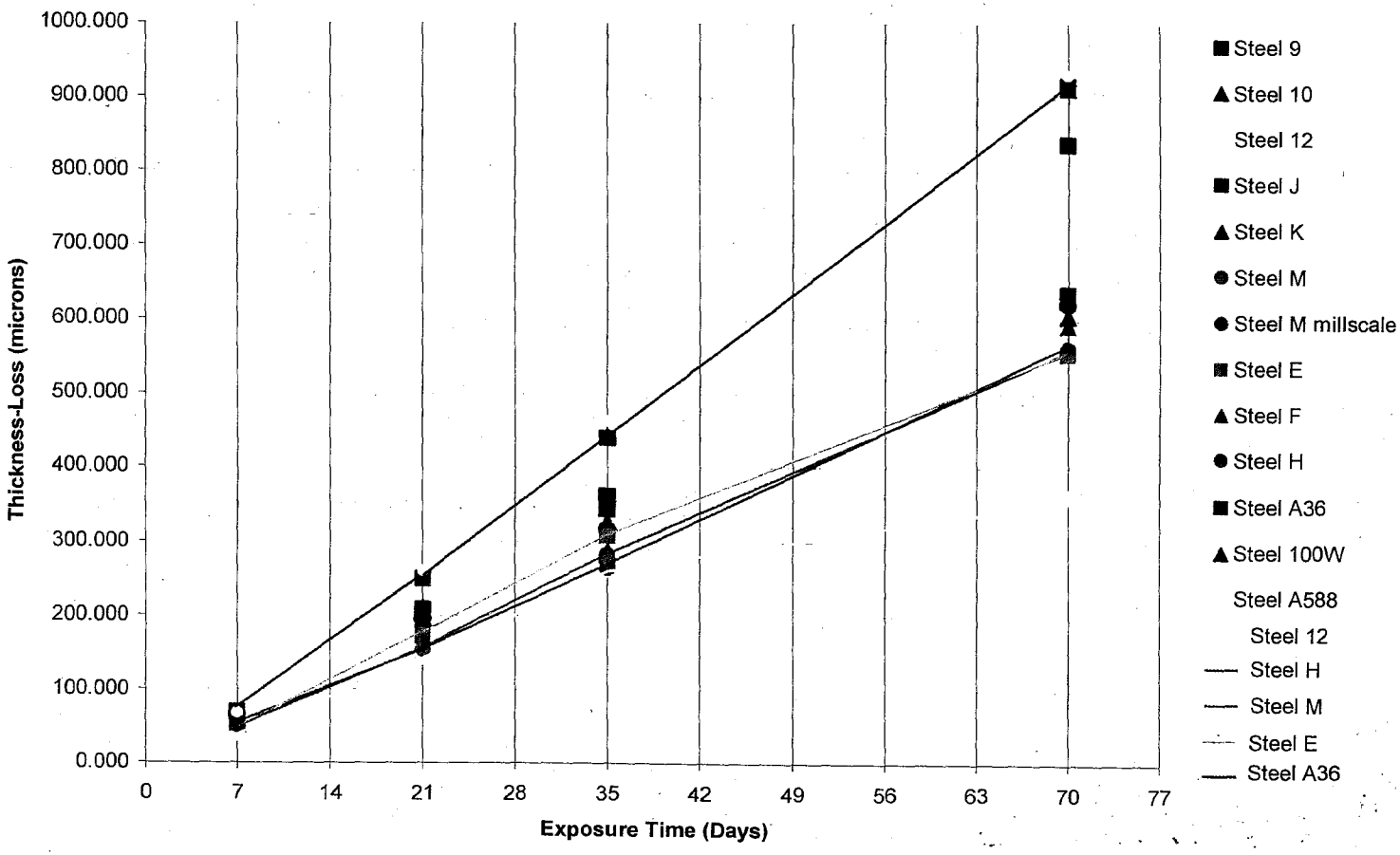

Figure 15 – Thickness-Loss Data

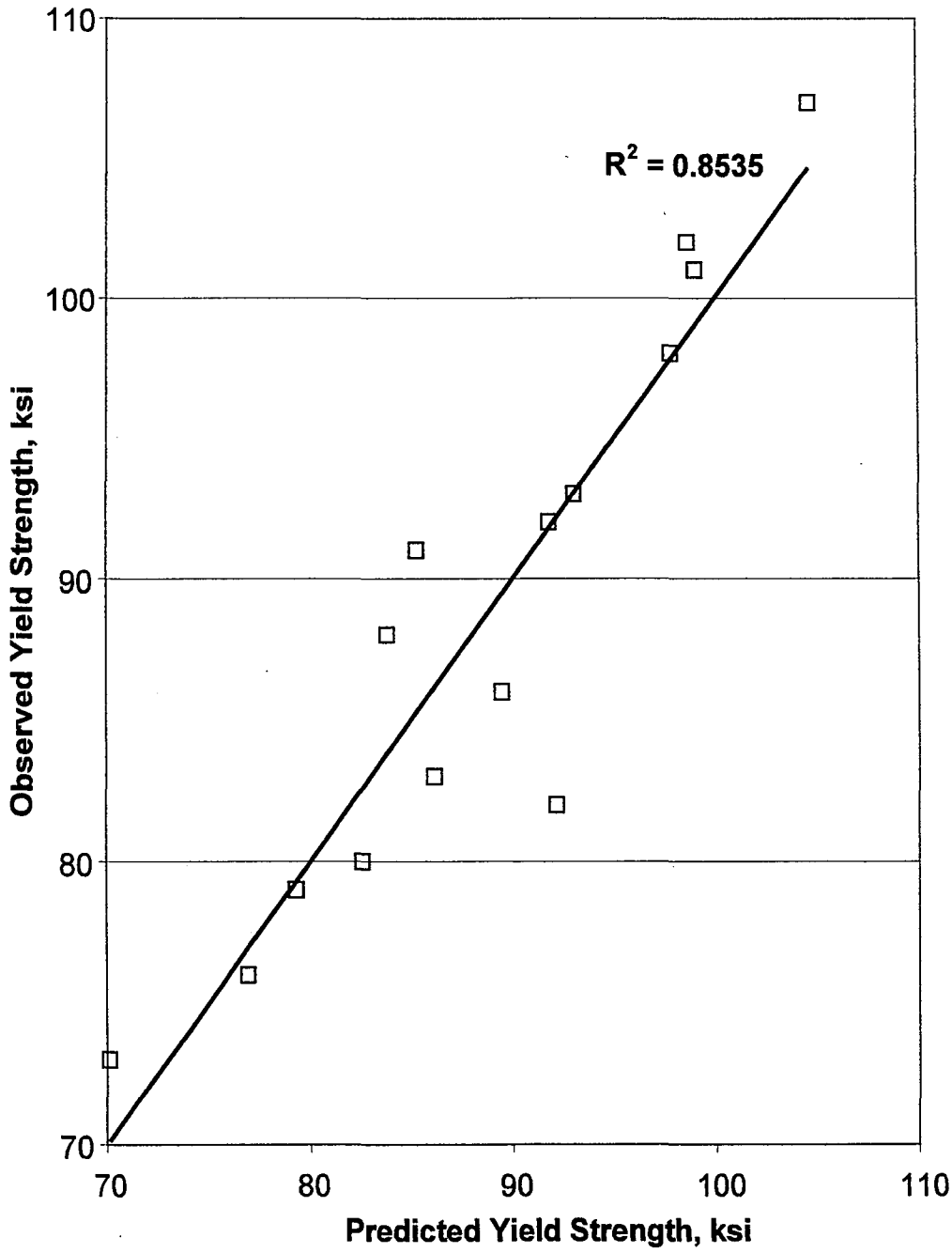

Figure 16 – Prediction of Yield Strength from Observed Data Equation

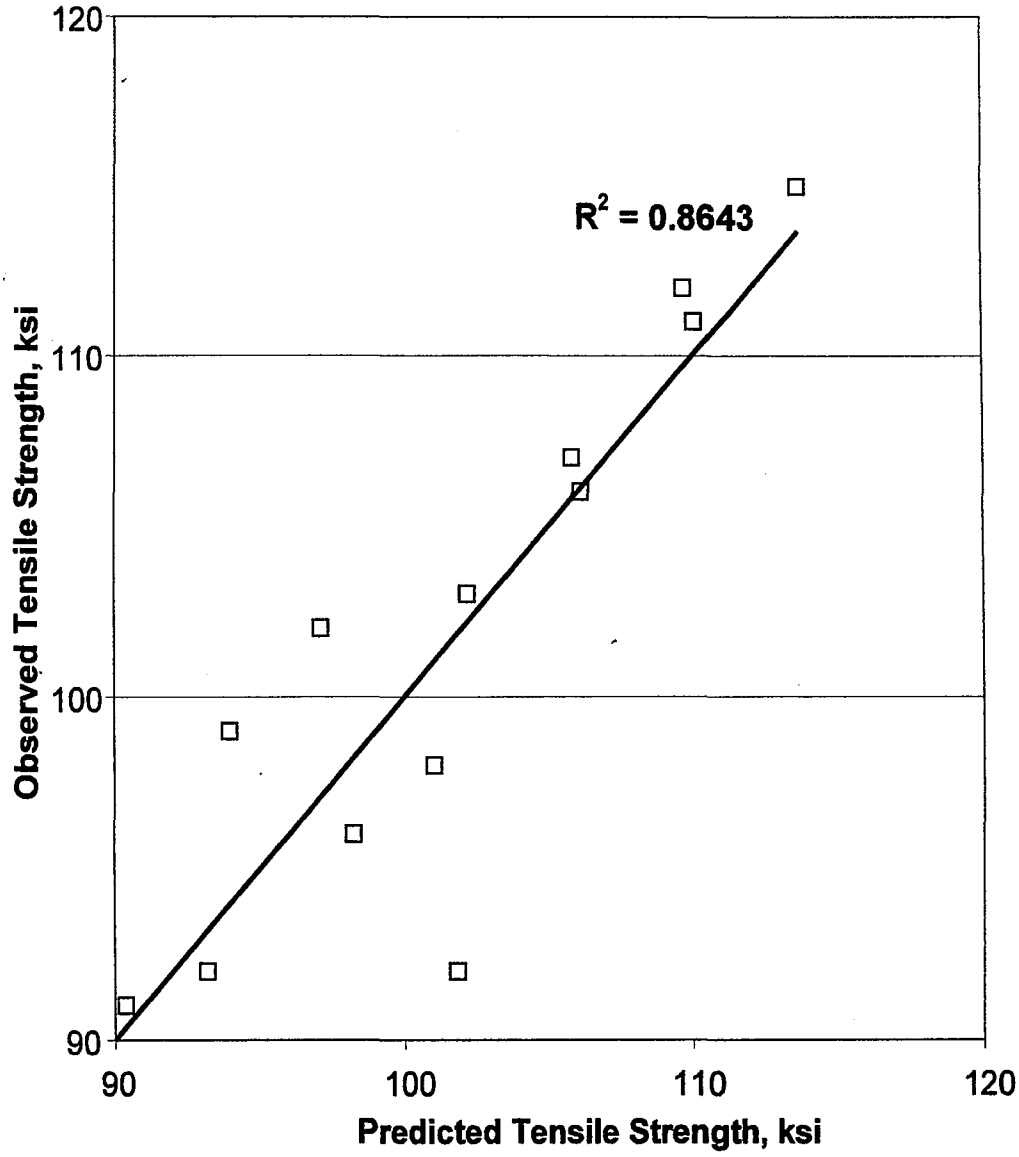

Figure 17– Prediction of Tensile Strength from Observed Data Equation

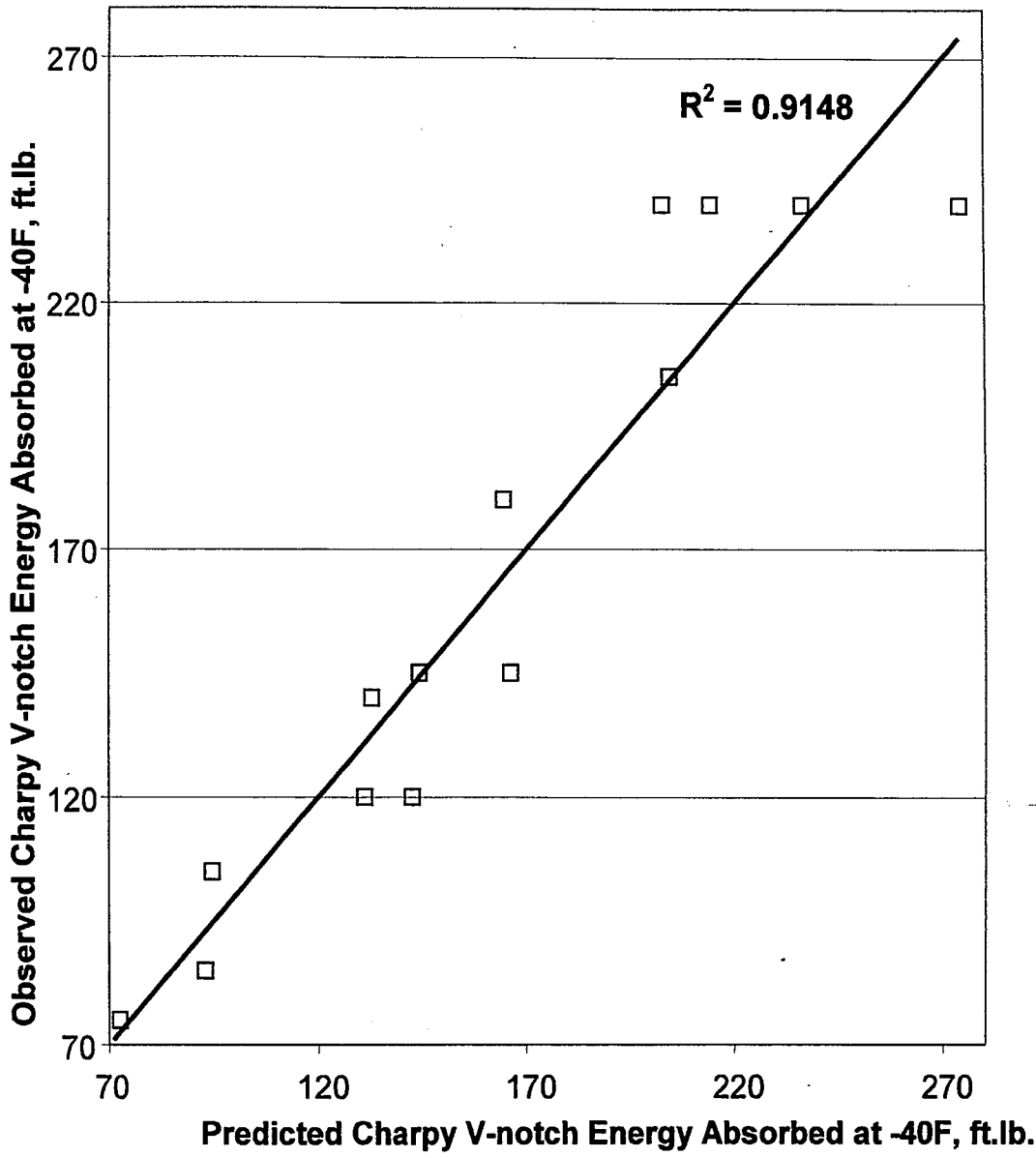

Figure 18 – Prediction of Charpy V-notch Energy Absorption from Observed Data Equation

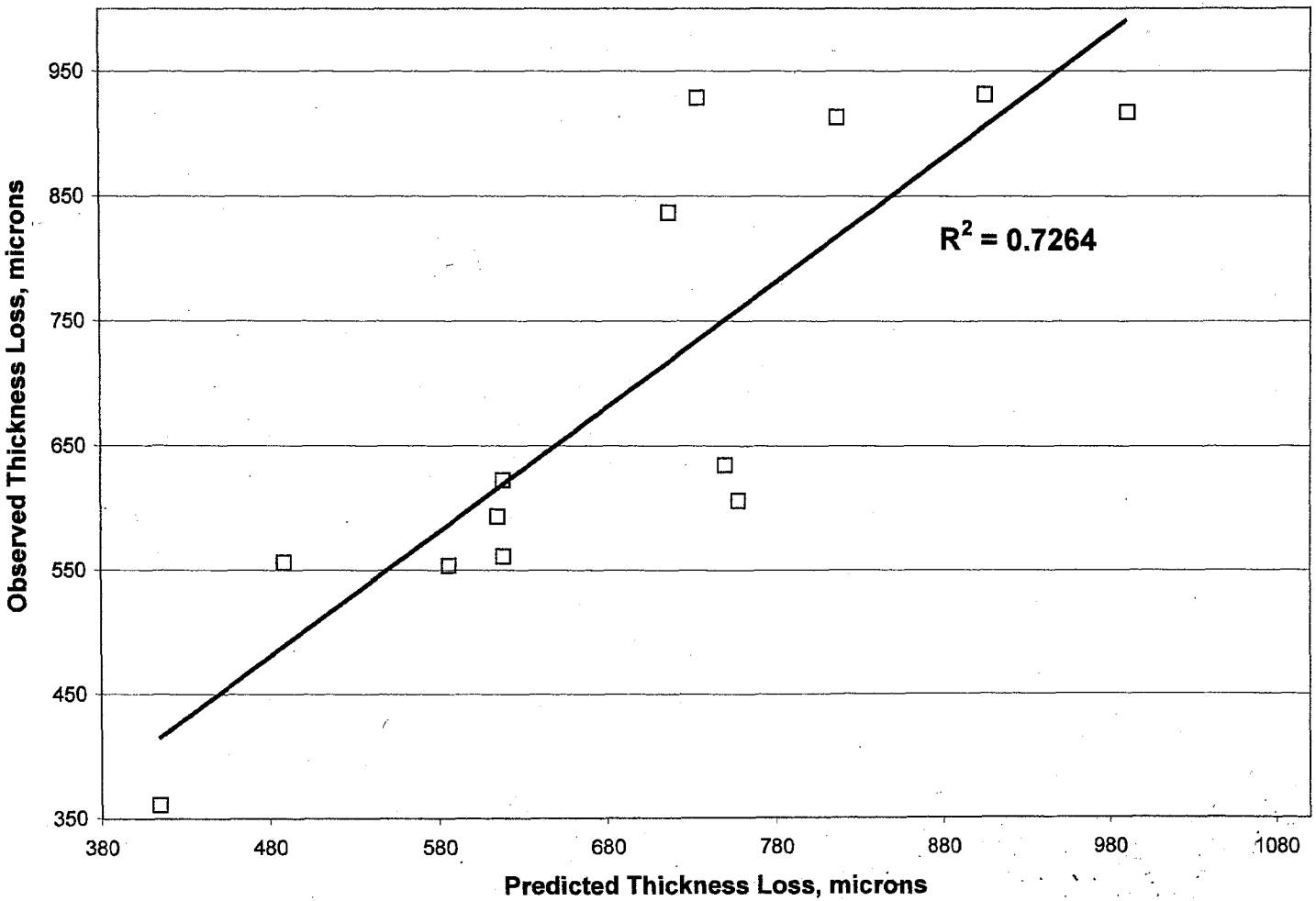

Figure 19 – Prediction of Thickness-Loss from Observed Data Equation

Illustration 1 – Omaha, Nebraska HPS100W Highway Bridge

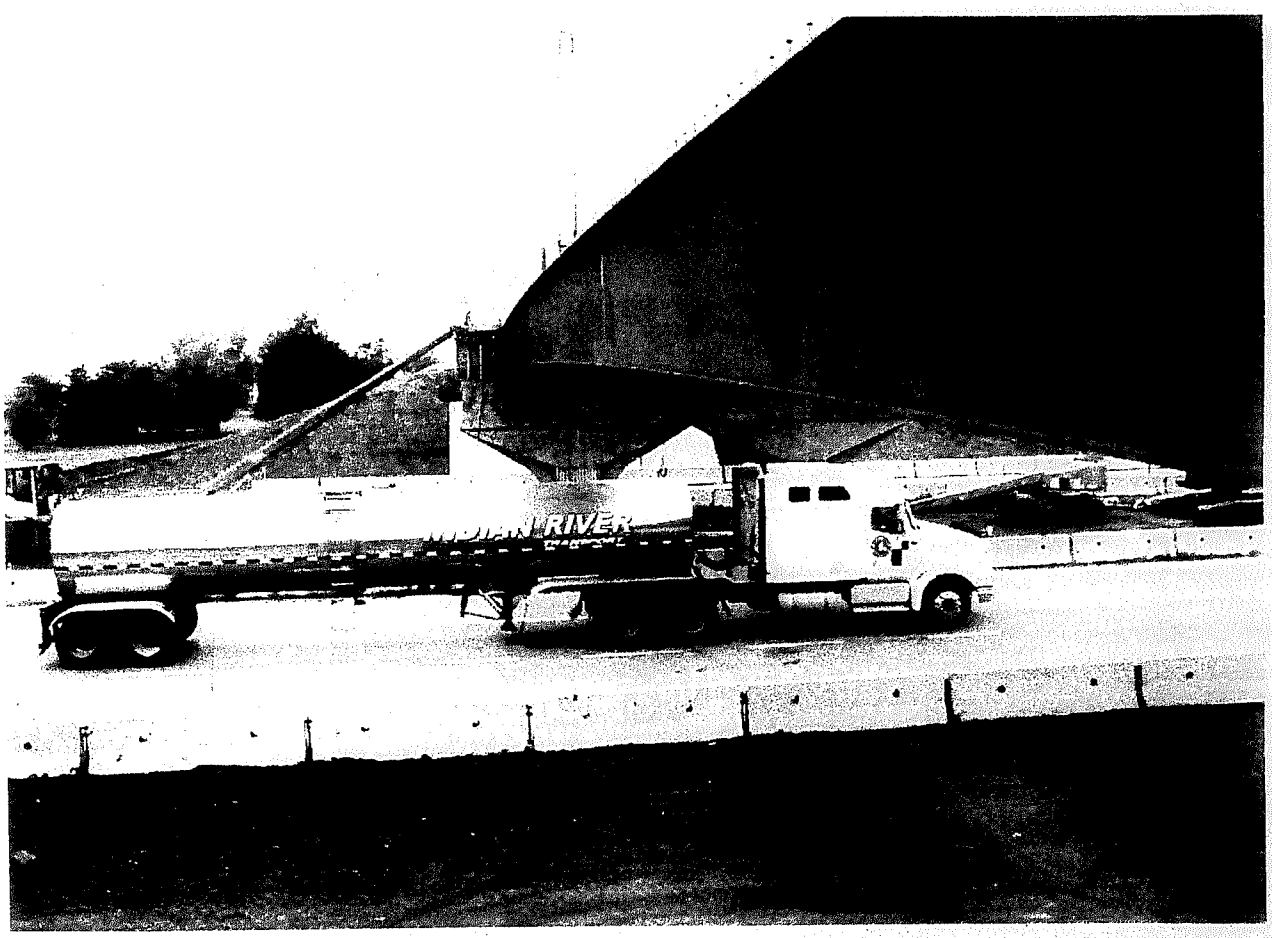

Illustration 1 – Omaha, Nebraska HPS100W Highway Bridge

REFERENCES

1. Broad Agency Announcement. "Improved Corrosion Resistant Steel for Highway Bridge Construction." Federal Highway Administration Presolicitation Notice No. DTFH61-06-R-00024, May 2006.

2. Cano, Oscar H. "New Developments in Low Corrosion Economical Construction Products." Annual Quality Congress Transactions. Milwaukee, WI: American Society for Q, 2001: 4-16

3. Virmani, Y.P. Corrosion Costs and Preventive Strategies in the United States. Federal Highway Administration Technical Report No. FHWA-RD-01-156, March 2002. p.773.

4. Sause, R. and A.W. Pense. "Cost Effective Bridge Design Using High Performance Steels (HPS)." International Symposium on Steel for Fabricated Structures. Materials Solutions, 1999. Materials Park, OH. ASM International, 1999: 3-10.

5. Kage, Isamu, et al. "Minimum Maintenance Steel Plates and Their Application Technologies for Bridge—Life Cycle Cost Reduction Technologies with Environmental Safeguards for Preserving Social Infrastructure Assets—." JFE Technical Report, No.5. March 2005. p. 37-44.

6. Peart, John W. "Unpainted Weathering Steel Bridges: Corrosion Mechanisms and Maintenance Alternatives." Journal of Protective Coatings & Linings. Federal Highway Administration, Vol. 8. Issue 1. 1991: 36-42.

7. Kan, T, et al. "Development of Low Carbon-High Phosphorus Steel Plate with Superior Atmospheric Corrosion Resistance." SEAISI Quarterly. Vol. 15. Issue 2. 1986: 27-35.

8. "The New Steel." Bethlehem Steel. 2000.

9. Cook, Desmond C. "Spectroscopic identification of protective and non-protective corrosion coatings on steel structures in marine environments." Corrosion Science. Vol. 47. Issue 10. October 2005. p. 2550-2570.

APPENDIX

1. Dawson, H.M and J.H. Gross, R.D. Stout. "Copper-Nickel High Performance 70W/100W Bridge Steels-Part I." ATLSS Report No. 97-10. August 1997.

2. Gross, J.H. and R.D. Stout, H.M. Dawson. "Copper-Nickel High Performance 70W/100W Bridge Steels-Part II." ATLSS Report No. 98-02. May 1998.

3. Gross, J.H. and R.D. Stout. "Evaluation of a Production Heat of an Improved Cu-Ni 70W/100W Steel." ATLSS Report No. 01-10. June 2001.

4. Gross, J.H. and R.D. Stout. "Proposed Specification for a HPS 100W Cu-Ni Age-Hardening ASTM A709 Grade Bridge Steel." ATLSS Report No. 01-15. November 2001.

5. Gross, J.H. and R.D. Stout. "Weldability Evaluation of Cu-Ni HPS 100W Bridge Steel." ATLSS Report No. 03-13. July 2003.

6. Gross, J.H. and R.D. Stout. "Addendum to Weldability Evaluation of Cu-Ni HPS 100W Bridge Steel." ATLSS Report No. 03-29. December 2003.

7. Dawson, H.M and J.H. Gross, R.D. Stout. "Effect of Copper on the Properties of Cu-Ni Structural Steels." ATLSS Report No. 99-08. November 1999.

8. Dawson, H.M and J.H. Gross, R.D. Stout. "Effect of Nickel on the Properties of Cu-Ni Structural Steels." ATLSS Report No. 99-09. December 1999.

9. Gross, J.H. and R.D. Stout. "Atlas of Transformation Characteristics for Precipitation-Strengthened Cu-Ni Infrastructure Steels." ATLSS Report No. 04-20. September 2004.

10. Gross, J.H. and R.D. Stout. "Evaluation of a Proposed Composition of a Cu-Ni HPS 120W Steel." ATLSS Report No. 06-02. January 2006.

Vita

Kate Arico was born in New Brunswick, NJ on July 23, 1984. She is the daughter of Thomas and Kathy Arico. Kate graduated from Hunterdon Central Regional High School in June 2002 and entered Lehigh University in Bethlehem, PA that fall. She graduated with Honors from Lehigh University receiving a Bachelor of Science degree in Industrial Engineering in May 2006. She was a member of the Lehigh University Division I softball team and the Industrial Engineering Honor Society, Alpha Pi Mu. During her college career, Kate received the Class of 1904 Scholarship for promise of future leadership, extracurricular activities, and character. She also received the Elizabeth Major Nevious Award on the basis of leadership, citizenship, and scholarship.

She continued her education at Lehigh University with the goal of earning a Master of Science degree in Industrial Engineering in January of 2008. While working toward her Master of Science degree, Kate was a Research Associate at the Advanced Technology for Large Structural Systems (ATLSS) Center located at Lehigh. Her responsibilities included conducting metallurgical testing and multivariable regression analysis to correlate experimental steel compositions with various results from hardenability, mechanical properties, weldability, and corrosion tests.

END OF TITLE